ornl

ORNL/TM-13200

OAK RIDGE NATIONAL LABORATORY

LOCKHEED MARTIN

Chemical Modeling of Waste Sludges

C. F. Weber
E. C. Beahm

MANAGED AND OPERATED BY
LOCKHEED MARTIN ENERGY RESEARCH CORPORATION
FOR THE UNITED STATES
DEPARTMENT OF ENERGY

ORNL-27 (3-96)

ORNL/TM-13200

Chemical Technology Division

CHEMICAL MODELING OF WASTE SLUDGES

C. F. Weber* and E. C. Beahm

Date Published: October 1996

*Computational Physics and Engineering Division

Prepared by the
OAK RIDGE NATIONAL LABORATORY
managed by
LOCKHEED MARTIN ENERGY RESEARCH CORP.
for the
U.S. DEPARTMENT OF ENERGY
under contract DE-AC05-96OR22464

CONTENTS

LIST OF FIGURES

LIST OF TABLES

ABSTRACT

This report describes the development and application of chemical thermodynamic models to electrolyte systems as are commonly encountered in waste tank sludges. The system Na-K-Ca-H-NO_3-OH-Cl-H_2O is modeled at 25°C using Pitzer's ion-interaction approach. All relevant binary and ternary parameters not available in the literature are determined primarily from common-ion isopiestic or solubility data. In addition, free energies of formation for important solid species are chosen so as to closely match the solubility data. A variation of the SOLGASMIX code is used to calculate chemical equilibria for both parameter optimization and simulation. The optimal parameters are combined with literature data to form a data set for tank sludge chemistry. Calculations at 25°C of initial species distributions and acid leaching behavior for the MV25 tank at ORNL are compared with analytical data. Parameter optimization is also applied to obtain a crude model of uranyl hydrolysis.

1. INTRODUCTION

The processing of waste from underground storage tanks at the Oak Ridge National Laboratory (ORNL) and other facilities will require an understanding of the chemical interactions of the waste with process chemicals. Two aspects of sludge treatment should be well delineated and predictable: (1) the distribution of chemical species between aqueous solutions and solids, and (2) potential problems due to chemical interactions that could result in process difficulties or safety concerns.

It is likely that the treatment of waste tank sludge will begin with washing, followed by basic or acidic leaching. The dissolved materials will be in a solution that has a high ionic strength where activity coefficients are far from unity. Activity coefficients are needed in order to calculate solubilities. Several techniques are available for calculating these values,[1] and each technique has its advantages and disadvantages. The techniques adopted and described here is the Pitzer method. Like any of the methods, prudent use of this approach requires that it be applied within concentration ranges where the experimental data were fit, and its use in large systems should be preceded by evaluating subsystems.

While much attention must be given to the development of activity coefficients, other factors such as coprecipitation of species and Ostwald ripening must also be considered when one aims to interpret results of sludge tests or to predict results of treatment strategies. An understanding of sludge treatment processes begins with the sludge tests themselves and proceeds to a general interpretation with the aid of modeling. One could stop with only data from the sludge tests, in which case the table of data would become an implicit model.[2] However, this would be a perilous approach in situations where processing difficulties could be costly or result in concerns for the environment or health and safety.

2. DEVELOPMENT OF AQUEOUS SOLUTION MODELS

One of the primary uses of electrolyte thermodynamics is the prediction of salt solubilities. This is certainly the case with natural water, which has such diverse applications as the precipitation of natural mineral deposits and the desalination of seawater. The principal components in such analyses are Na^+ and Cl^-, with Mg^{2+} and SO_4^{2-} being secondarily important.

Describing the behavior of components in low-level liquid waste sludges is similar to modeling precipitation processes in natural waters. The basic ideas of chemical activity and solubility apply in both areas. Specific models for activity coefficients are relevant in both, as are the common experimental approaches and even the resulting data. Sometimes geochemists need to be concerned with very high pressures and temperatures, which are generally not applicable in waste sludge studies. Most tank contents have been processed through industrial evaporators, which have no doubt exceeded 100°C at ambient pressure; hence, comprehensive sludge modeling should cover this temperature range. However, this study is a preliminary step to thoroughly characterize the desired electrolyte systems at room temperature. Thus all data, parameter values, and simulations occur at 25°C unless otherwise noted. The primary components in sludges usually include the four cations

Na^+, K^+, Ca^{2+}, and Mg^{2+}, as well as the anions NO_3^-, OH^-, CO_3^{2-}, SO_4^{2-}, and PO_4^{3-}. In addition, the importance of sludge modeling is driven by the many minor (in mass) components, which may be radioactive or environmentally hazardous. The primary goal is to predict distributions between liquid and precipitate for each element of environmental importance.

3. REVIEW OF ELECTROLYTE THERMODYNAMICS

If an aqueous solution containing ions M and X is in equilibrium with the solid precipitate MX, then the distribution is described by the solubility product. For the case of singly charged ions, this quantity is

$$K_{sp} = a_M a_X = m_M m_X \gamma_{\pm}^2, \tag{1}$$

where a and m denote activity and molality, respectively, and $\gamma_{\pm}$ is the binary activity coefficient. (Generally, we will use M,N to denote positive ions, and X,Y to denote negative ions; the salts are represented by MX, NX, MY, and NY.) The formulation for $\gamma_{\pm}$ used by refs. 3–5 involves a Debye-Hückel term and power series in I, the ionic strength:

$$\ln \gamma = - \frac{A\sqrt{I}}{1 + B\sqrt{I}} + CI + DI^2 + EI^3 + \ldots . \tag{2}$$

The activity of water is most conveniently represented by the osmotic coefficient[6]

$$\phi = - \frac{\Omega}{\Sigma m_i} \ln a_{H_2O}, \tag{3}$$

where $\Omega = 55.508$ mol/kg. By using this definition and the Gibbs-Duhem equation, it can be shown[3] that the following representation is consistent with Eq. (2):

$$\phi - 1 = \frac{A}{B^3 I}[-(1 + B\sqrt{I}) + 2\ln(1 + B\sqrt{I}) + (1 + B\sqrt{I})^{-1}] + \frac{1}{2}CI + \frac{2}{3}DI^2 + \frac{3}{4}EI^3 + \ldots . \tag{4}$$

In Eqs. (2) and (4), the coefficient A depends on the Debye-Hückel constant, known for given temperature and solution components and the ionic charges ($A = 1.17616$ for singly charged ions at 25°C). The coefficients B, C, D, . . . are obtained for each electrolyte from statistical fitting of data. As many parameters as necessary can be used to represent activity and osmotic coefficients accurately

through extremely wide ranges of ionic strength, in some cases exceeding $I = 20$. Table 1 lists the values of these coefficients for several electrolytes of interest.

Within the past 20 years, the procedure used by Pitzer and coworkers[6,7] has become quite popular. For a binary system (i.e., a solution containing only one anion and one cation), the analogs of Eqs. (2) and (4) are

$$\ln \gamma_{\pm} = -A_1 |z_m z_x| \left[\frac{\sqrt{I}}{1 + b\sqrt{I}} + \frac{2}{b} \ln(1 + b\sqrt{I}) \right] + m \frac{2\nu_M \nu_X}{\nu} B^{\gamma} + m^2 \frac{2(\nu_M \nu_X)^{\frac{3}{2}}}{\nu} C^{\gamma}, \quad (5)$$

and

$$\varphi - 1 = -\frac{A_1 |z_m z_x| \sqrt{I}}{1 + b\sqrt{I}} + m \frac{2\nu_M \nu_X}{\nu} B^{\varphi} + m^2 \frac{2(\nu_M \nu_X)^{\frac{3}{2}}}{\nu} C^{\varphi}, \quad (6)$$

where A_1 is the modified Debye-Hückel constant, $b = 1.2$ is a fixed constant, and ν_M, ν_X, $\nu = \nu_M + \nu_X$ are stoichiometric constants. The terms B^{γ}, B^{φ}, C^{γ}, and C^{φ} depend on the adjustable parameters β^0, β^1, and C (which are fit to data) according to the relations

$$B^{\varphi} = \beta^0 + \beta^1 e^{-\alpha\sqrt{I}}, \quad B = \beta^0 + \beta^1 g(\alpha\sqrt{I}), \quad g(x) = \frac{2}{x^2}[1 - (1 + x)e^{-x}]$$

and

$$B^{\gamma} = B + B^{\varphi}, \quad C^{\varphi} = 2|z_M z_X| C, \quad C^{\gamma} = \frac{3}{2} C^{\varphi}.$$

The constant $\alpha = 2$ (kg/mol)$^{1/2}$ is fixed; z_M and z_X are the ionic charges. While the Pitzer formulation is usually applicable only in the range $0 < I < 6$, it requires only three adjustable parameters and is, therefore, easier to use than Eqs. (2) and (4). In addition, the Pitzer formulation is easily generalized to multicomponent solutions (unlike the method of Hamer and Wu), which is one reason for its popularity. The adjustable parameters have been determined for many electrolytes (see ref. 6). In addition, Kim and Frederick[8,9] have derived alternative binary representations to cover ranges of high ionic strength, although their parameters do not model well at lower values of I.

3.1 PITZER'S METHOD IN MULTICOMPONENT SOLUTIONS

The Pitzer formulation has its primary strength in accuracy using only a few parameters. For many applications, the three binary system parameters (β^0, β^1, and C) will provide a credible

Table 1. Activity and osmotic coefficient parameters[a]

Salt	*B*	*C*	*D*	*E*	*F*	*G*	*H*
HCl	1.525	0.24163	0.01505	–9.6842E-4	–9.3715E-6	1.2107E-6	
HNO_3	1.5824	0.14375	–0.0030249	–2.9625E-5	1.13214E-6		
NaCl	1.4495	0.047069	0.013338	–6.6453E-4			
$NaNO_3$	1.2053	–0.070055	0.0055519	–1.9221E-4			
NaOH	1.21	0.14163	–0.006858	3.0608E-3	–2.5637E-4	8.1631E-6	-9.2069E-8
KCl	1.295	1.6118E-4	0.008287	–4.4993E-4			
KNO_3	0.975	-0.23233	0.015661				
KOH	1.15	0.23026	0.0060489	–2.9934E-4	3.9144E-7		

[a]Values obtained from refs. 3 and 4.

description of behavior in systems containing more than just a single cation-anion pair. However, this is not always the case, and a few additional parameters may be necessary. The "mixing rules" of the Pitzer procedure are best illustrated with a ternary system (i.e., two salts that have a common anion or a common cation). In a solution of salts MX and NX, the activity and osmotic coefficients can be represented as

$$\nu \ln \gamma_{MX} = \nu|z_M z_X|F + 2B_{MX}(\nu_X m_M + \nu_M m_X) + C_{MX}[Z(\nu_M m_X + \nu_X m_M) + 2\nu_M z_M m_M m_X]$$
$$+ 2\nu_X m_N B_{NX} + m_N C_{NX}(\nu_X Z + 2m_X \nu_M z_M) + 2m_N \nu_M \Phi_{MN} + m_N \psi_{MNX}(m_M \nu_X + m_X \nu_M) \quad (7)$$

and

$$\frac{1}{2}(m_M + m_N + m_X)(\varphi - 1) = If^{\varphi} + m_M m_X(B^{\varphi}_{MX} + ZC_{MX})$$
$$+ m_N m_X(B^{\varphi}_{NX} + ZC_{NX}) + m_M m_N(\Phi^{\varphi}_{MN} + m_X \psi_{MNX}) \; . \quad (8)$$

Quantities in the above are defined as

$$F = f^{\gamma} + m_M m_X B'_{MX} + m_N m_X B'_{NX} + m_M m_N \Phi'_{MN}$$

$$Z = m_M z_M + m_N z_N - m_X z_X$$

where prime denotes differentiation with respect to ionic strength; f^{γ} and f^{φ} are the Debye-Hückel terms in Eqs. (5) and (6):

$$f^{\varphi} = -\frac{A_1\sqrt{I}}{1 + b\sqrt{I}}, \quad f^{\gamma} = f^{\varphi} - \frac{2A_1}{b}\ln(1 + b\sqrt{I}) \; .$$

If both MX and NX are 1–1 salts, then these can be expressed in terms of binary activity and osmotic coefficients, together with "mixing terms" involving Φ and ψ. To begin, the binary system representations (5) and (6) can be expressed as

$$\ln \gamma^{b}_{MX} = f^{\gamma} + IB^{\gamma}_{MX} + I^2 C^{\gamma}_{MX} \quad (9)$$

and

$$\varphi^{b}_{MX} - 1 = f^{\varphi} + IB^{\varphi}_{MX} + I^2 C^{\varphi}_{MX}, \qquad (10)$$

where the superscript "b" is now used to indicate the binary solution representation. Analogous expressions also hold for the binary solution of salt NX. For 1–1 salts, Eqs. (7) and (8) can be rearranged and expressed in terms of Eqs. (9) and (10):

$$\ln \gamma_{MX} = \ln \gamma^{b}_{MX} + y(\varphi^{b}_{NX} - \varphi^{b}_{MX}) + yI[\Phi_{MN} + I(1 - \frac{y}{2})\psi_{MNX})] \qquad (11)$$

and

$$\varphi - 1 = y(\varphi^{b}_{MX} - 1) + (1 - y)(\varphi^{b}_{NX} - 1) + y(1 - y)I(\Phi_{MN} + I\psi_{MNX}) \; . \qquad (12)$$

Equations (11) and (12) are useful since they identify those mixing rules which utilize the parameters Φ_{MN} and ψ_{MNX} and involve general binary solution activity and osmotic coefficients. The special nature of Eqs. (11) and (12) does not require use of Pitzer binary representations (9) and (10), nor even knowledge of the binary parameters β^0, β^1, and C for salts MX and NX. That is, some other formalism for binary coefficients [e.g., Eqs. (2) and (4)] can be used to estimate the Pitzer mixing parameters Φ_{MN} and ψ_{MNX}. This is especially helpful if the range of ionic strength exceeds that for which the binary Pitzer parameters are valid (generally $I \leq 6$). It is important also to note that Eqs. (11) and (12) were derived for a 1–1 electrolyte. Such simple relations do not hold generally unless $\nu_M = \nu_N = \nu_X$. However, similar results can also be obtained for ternary 1–1 systems involving a common cation.

3.2 USE OF SOLUBILITY DATA

One of the motivations for the developments outlined above is to be able to estimate Pitzer mixing parameters by using solubility data of high ionic strength. Harvie and coworkers[10-12] have demonstrated the ability to estimate mixing parameters using solubility data of moderate ionic strengths (usually $I < 6\ m$). At higher ionic strengths, the results may not be applicable generally, since the error in the binary parameters may contribute to significant error in the mixing terms. They were primarily concerned with natural waters in which Na^+ and Cl^- are the dominant ions, while we are concerned with solutions high in $NaNO_3$, whose solubility is near 11. Furthermore, some of the other mixed solutions we shall consider have ionic strengths well into the teens, possibly exceeding $I = 20\ m$. Thus we hope to apply Eqs. (11) and (12) using binary representations (2) and (4) in order to evaluate Pitzer mixing parameters Φ and ψ from solubility data at high ionic strengths, far higher than the valid range of the binary Pitzer parameters β^0, β^1, and C.

A second problem that arises is the limitation on binary parameters due to the solubility limit of the binary salt. For example, KNO_3 has a solubility of about 3.8 *m*, although binary solution data only go to 3.5 *m*. Any estimation of binary solution parameters that use only these data will decrease in validity if applied to solutions where I increases above 3.5 *m*. In many applications (including our sludge processing), we expect ionic strengths in the 5–6 *m* range; hence, it is desirable to extend the range of applicability for binary parameters by using data from ternary systems. [This problem is even more obvious for sparingly soluble salts such as $Ca(OH)_2$ and $CaCO_3$.] However, there must be some way to separate the effects of modified binary parameters from the effects of mixing parameters. This issue requires that if binary parameters are to be estimated, at least two (and preferably more) mixed solutions should be considered.

4. PARAMETER ESTIMATION

4.1 MATHEMATICAL FORMULATION

Solubility data can be expressed as the molality of each ion in a solution that is at equilibrium with a pure solid salt. The presence of a third ion will affect the activity coefficient in Eq. (1) through the ionic strength. If $\hat{m}_M$, $\hat{m}_N$, and $\hat{m}_X$ represent experimental data in equilibrium with salt MX, then $\hat{I} = \frac{1}{2}(\hat{m}_M + \hat{m}_N + \hat{m}_X)$ is the experimental ionic strength. If $\gamma_\pm$ is calculated at this ionic strength, then the experimental solubility product is

$$\hat{K}_{sp} = \hat{m}_M \hat{m}_N \gamma_\pm^2(\hat{I}) \ . \tag{13}$$

For a given temperature and pressure, the solubility product should be constant, regardless of how constituent molalities change. If the best estimate of the solubility product is K_{sp}, then the logarithmic error is

$$\epsilon = \ln K_{sp} - \ln \hat{K}_{sp} = \ln K_{sp} - \ln \hat{m}_M \hat{m}_N - 2 \ln \gamma_\pm(\hat{I}) \ . \tag{14}$$

For several solubility measurements involving the same solution components, we form the sum of squared error

$$SSE_1 = \Sigma \epsilon_i^2 \ , \tag{15}$$

where ϵ_i is the error [cf. Eq. (14)] of the *i*th solubility measurement. If several sets of solubility data are used, each will have its own solubility product constant and error sum. The total solubility error is then

$$SSE_1 = SSE_{1a} + SSE_{1b} + \ldots .$$

Thus a given choice of solubility product constant and activity coefficient parameters will yield a certain sum of squared error via Eq. (15). If the representation (2) is used for the binary activity coefficients, then we desire to minimize SSE_1 through judicious choice of K_{sp}, B, C, D, . . ., and perhaps Φ_{MN} and ψ_{MNX} as well.

It is also important that activity coefficients are accurately modeled below the binary solution solubility limit. This can be done by selecting various data points from the binary solution

$$\hat{f}_i = \ln \hat{\gamma}_{\pm i}, \quad \hat{g}_i = \hat{\varphi}_i, \text{ at } I = \hat{I}_i .$$

Any representation utilizing B, C, D, . . . to model solubility behavior will yield binary activity and osmotic coefficients through Eqs. (2) and (4). If we call these f_i and g_i, respectively, the resulting sums of squared error are

$$SSE_2 = \Sigma(f_i - \hat{f}_i)^2 , \quad SSE_3 = \Sigma(g_i - \hat{g}_i)^2 . \tag{16}$$

In some applications, it may be desirable to weight certain residuals higher than others; however, most results presented involve equal weights for all error residuals.

Our basic mathematical formulation is obtained by combining Eqs. (15) and (16). That is, we seek parameters K_{sp}^a, K_{sp}^b, . . ., B, C, D, . . ., and possibly Φ_{MN}, ψ_{MNX}, whose values minimize the total sum of squared error

$$SSE = SSE_1 + SSE_2 + SSE_3 .$$

The least-squares problem formulated above is nonlinear, since the computed quantities ln K_{sp}, f_i, and g_i in Eqs. (15) and (16) depend nonlinearly on the problem parameters. Thus an iterative approach is necessary, whereby successive estimates of the parameters are used to generate a decreasing sequence of squared error sums. When small parameter changes no longer decrease the SSE, the optimal solution has been attained. A number of mathematical procedures have been proposed and can be found in standard references on optimization theory. The solution procedure used in this work involves both Gauss-Newton and quasi-Newton algorithms, following suggestions in ref. 13.

By using the special approach for 1–1 electrolytes, only activity (or osmotic) coefficients and solubility products are calculated and utilized to compute the residual squared error. In addition, the parameter uncertainty (standard deviation) σ is calculated using estimated data uncertainties. However, for all other systems, the actual phase equilibrium is calculated using the principal subroutines of the SOLGASMIX code; the resulting soluble molarities are then used to calculate the SSE.

4.2 RESULTS FOR 1–1 ELECTROLYTES

The actual estimation of parameters is straightforward, as described in the following subsections. We found it necessary to estimate parameters for some systems which are of little direct interest; however, they allowed us to include additional data in fitting parameters that are of interest to us. The following paragraphs describe a sequence of fitting runs that will eventually allow calculation of unknown, but necessary, Pitzer parameters. As mentioned previously, all data occur at 25°C. Unless stated otherwise, the standard states of all charged species are aqueous ions, and the standard states of noncharged species are crystalline solids.

4.2.1 NaCl to High Ionic Strengths

Although NaCl was not important per se, it enabled the subsequent calculation of other parameters more effectively. Using solubility data for the ternary systems Na-H-Cl, Na-Cl-OH, and Na-Cl-NO_3, we extended the range of NaCl binary parameters from the salt solubility limit (about 6.1 *m*) to ionic strengths of about 12. In lieu of actual experimental measurements, the published values of Hamer and Wu[3] for binary activity and osmotic coefficients were used as data points below the solubility limit [cf. Eq. (16)]. The results of parameter estimation are shown in Table 2. No ternary mixing parameters were included in the optimization since satisfactory values were already available, as listed in Table 2. Figures 1–3 illustrate the usefulness of these results in calculating solubilities.

4.2.2 KCl to High Ionic Strengths

Again, KCl was not very important per se but, rather, because it was useful in subsequent calculations. The binary parameters have been fit to data up to the solubility limit (about 4.8 *m*). This range is extended to ionic strengths of 9.3 by using solubility data for ternary systems K-H-Cl, K-Cl-OH, and K-Na-Cl. The published results of Hamer and Wu[3] were used in place of experimental data below the solubility limit. The parameter-fitting results are given in Table 3. Ternary mixing parameters $\psi_{K,H,Cl}$ and $\psi_{K,OH,Cl}$ were included in the optimization, and the resulting estimates differ somewhat from the values listed in ref. 6. The values in Table 3 allowed better computation of solubilities and, thus, were used in the remainder of this work.

4.2.3 $NaNO_3$ and KNO_3

Both $NaNO_3$ and KNO_3 are significant to the sludge modeling. Neither salt has been fully characterized; hence, estimates of several important mixing parameters resulted from this fitting. The two were optimized simultaneously because of the mixing parameter Φ_{OH,NO_3}, which is common to both K^+ and Na^+ systems. As mentioned previously, KNO_3 binary parameters are valid only up to I = 3.5. We wanted to extend this limit considerably. We also wanted to extend the range for $NaNO_3$ binary parameters and include several ternary mixing parameters. Again, binary results from Hamer and Wu[3] (revised values from Wu and Hamer[4] for $NaNO_3$) were used below the solubility limits. The resulting data set contained 188 data points. An initial optimization was performed, resulting in preliminary estimates of the parameters. A calculation based on these parameters produced the curve

Table 2. Optimal parameters for NaCl system[a,b]

Parameter	Value	σ
B	1.2508	0.17
C	0.12045	0.036
D	–0.014113	0.0075
E	0.0031755	0.00071
F	-1.6253×10^{-4}	0.24×10^{-4}
$\ln K_{sp}$(NaCl)	3.6155	0.0217

[a]Results valid to 12 *m*.

[b]Calculated using the following mixing parameters from Pitzer:[6] $\theta_{H,Na} = 0.036$, $\theta_{Cl,OH} = -0.050$, $\theta_{Cl,NO_3} = 0.016$, $\psi_{H,Na,Cl} = -0.004$, $\psi_{Na,Cl,OH} = -0.006$, and $\psi_{Na,Cl,NO_3} = -0.006$.

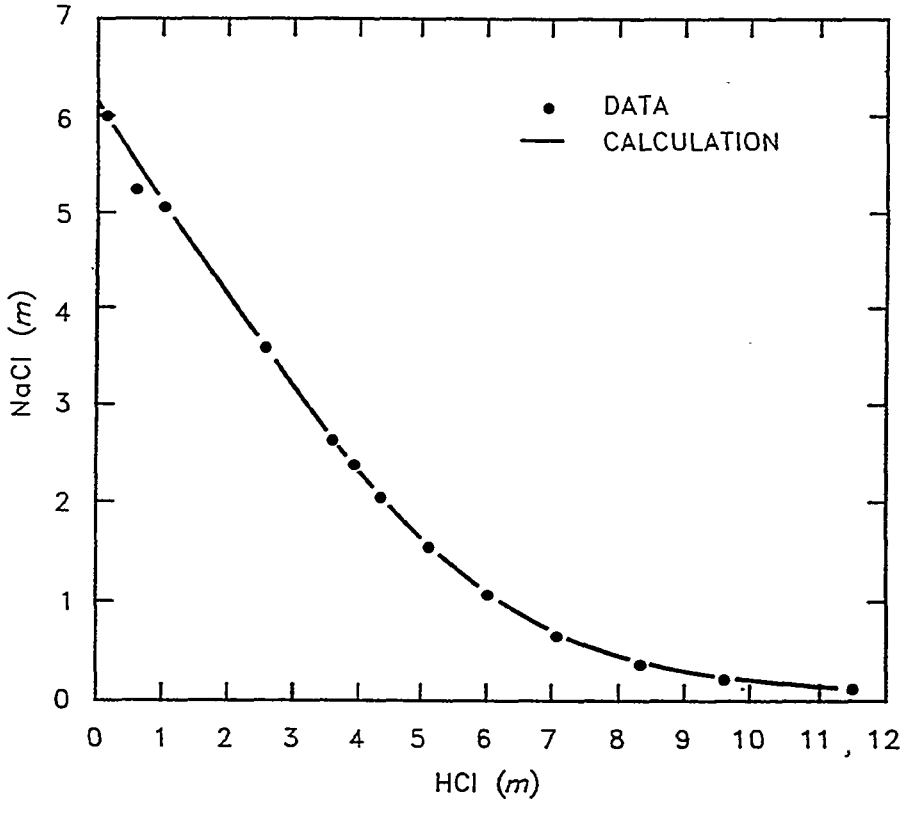

Fig. 1. Solubilities of NaCl in HCl solutions.

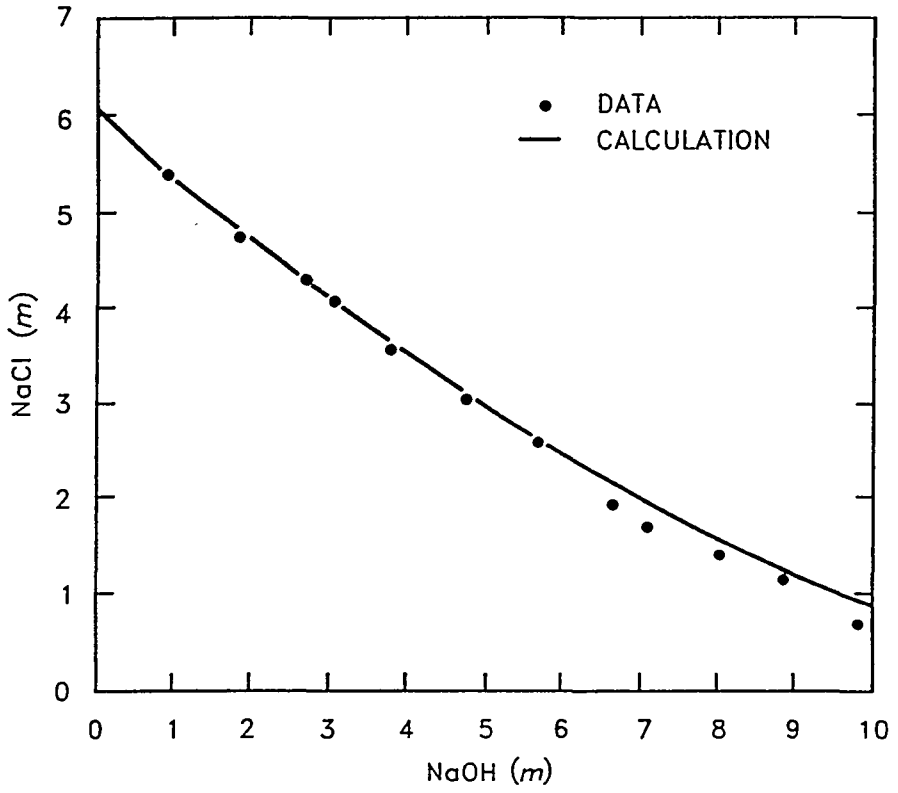

Fig. 2. Solubilities of NaCl in NaOH solutions.

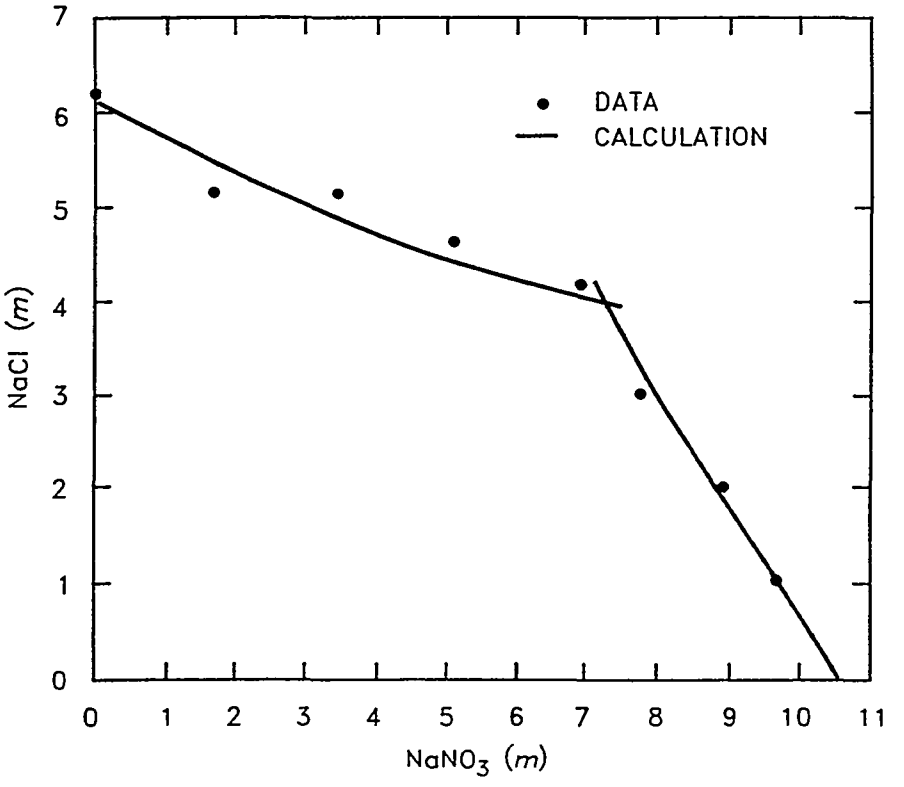

Fig. 3. Solubilities in the Na-Cl-NO_3 system.

Table 3. Optimal parameter values for KCl system[a,b]

Parameter	Value	σ
B	1.4391	0.0514
C	–0.050932	0.01325
D	0.034925	0.0044162
E	–0.0060853	0.00067
F	3.3275×10^{-4}	3.57×10^{-5}
$\ln K_{sp}$(KCl)	2.0148	0.00332
$\psi_{K,H,Cl}$	–0.01099	0.000099
$\psi_{K,OH,Cl}$	–0.00317	0.00010

[a]Results valid to 9.3 m.

[b]Calculated using the following mixing parameters from Pitzer:[6] $\theta_{K,H} = 0.005$, $\theta_{Cl,OH} = -0.050$, $\theta_{K,Na} = -0.012$, and $\psi_{K,Na,Cl} = -0.0018$.

in Fig. 4. (All other solubilities were adequately modeled.) The figure shows that while the curve closely approximates the given data, its odd shape betrays this as a spurious result, allowed only by the paucity of data. This problem was remedied by taking the five existing data points and exactly fitting a smooth curve through them using cubic spline interpolation,[14] as shown in Fig. 5. Several points on the interpolant curve were appropriated as additional data points for use in the parameter estimation. Use of these additional points resulted in the revised set of parameter estimates shown in Table 4. When the revised values were used, calculated solubilities more adequately represented the actual solubility circumstances, as shown in Fig. 6. The other calculated solubility curves are compared with data in Figs. 7–11. As shown, all calculated results are in excellent agreement with data, with the possible exception of the $NaNO_3$-KNO_3 system. Even for this system, calculated solubilities are adequate, especially considering the high ionic strengths involved.

4.2.4 Additional Derived Parameters

The results described in Tables 2–4 can be used to obtain additional quantities of interest. Free energies of formation for the solid species were obtained from the solubility products and free energies of the constituent ions. A sample calculation for NaCl is as follows:

$$\mu^0(\text{NaCl}) = \mu^0(\text{Na}^+) + \mu^0(\text{Cl}^-) + RT \ln K_{sp} \,. \qquad (17)$$

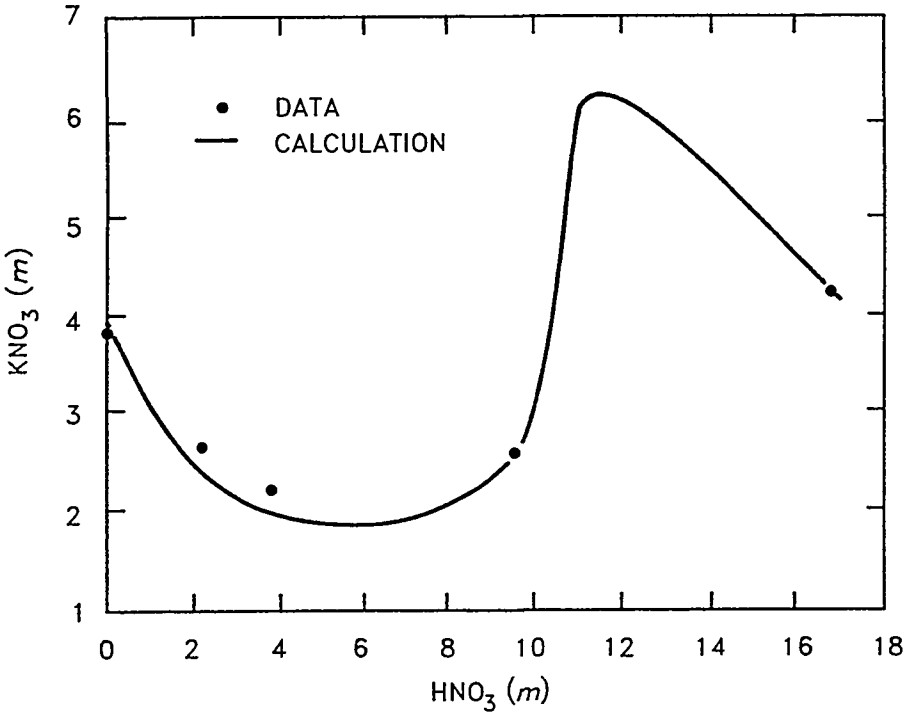

Fig. 4. Spurious model of KNO_3 solubilities in HNO_3.

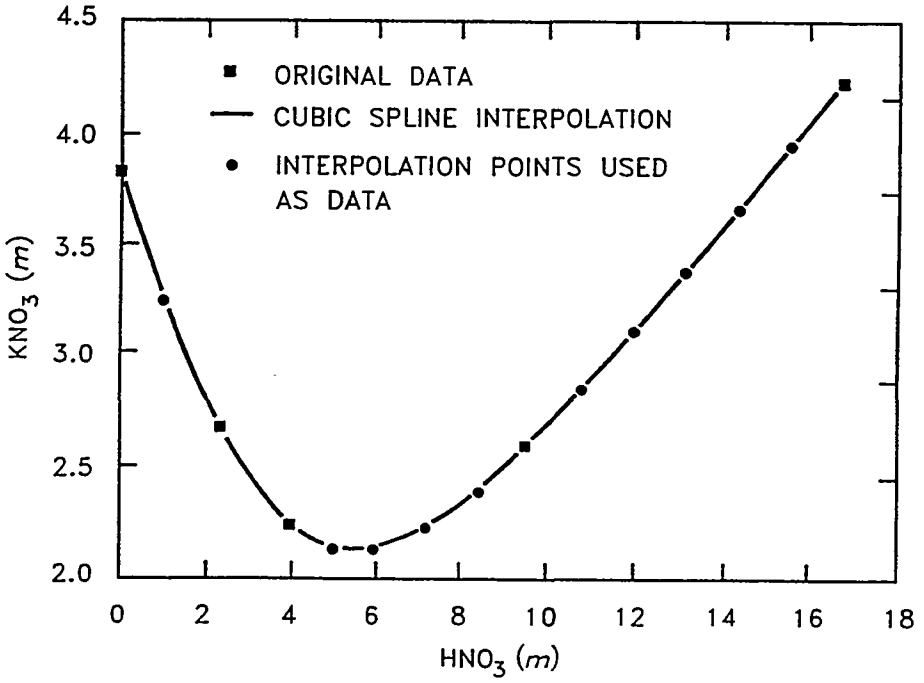

Fig. 5. Cubic spline interpolation of KNO_3 solubilities in HNO_3.

Table 4. Optimal parameters for nitrate system[a,b]

Parameter	Value	σ
$NaNO_3$		
B	1.2703	0.021
C	–0.091847	0.0039
D	0.0095787	0.00073
E	-3.7653×10^{-4}	0.68×10^{-4}
F	-3.3850×10^{-6}	2.9×10^{-6}
G	4.0644×10^{-7}	0.46×10^{-7}
$\ln K_{sp}$	2.5908	0.0028
KNO_3		
B	0.63579	0.025
C	–0.079415	0.012
D	–0.019942	0.0032
E	0.0038555	0.00043
F	-1.9745×10^{-4}	0.27×10^{-4}
G	3.8235×10^{-6}	0.62×10^{-6}
$\ln K_{sp}$	–0.19545	0.0087
Pitzer mixing parameters		
θ_{OH,NO_3}	–0.05466	0.00061
ψ_{K,OH,NO_3}	–0.00321	0.00039
ψ_{Na,OH,NO_3}	0.00019	0.00007
ψ_{K,H,NO_3}	–0.01034	0.00020
ψ_{Na,H,NO_3}	–0.00274	0.00001
ψ_{K,Cl,NO_3}	–0.00312	0.0064
ψ_{Na,K,NO_3}	–0.00596	0.00016

[a]Validity exceeds $I = 20$.

[b]Calculated using the following mixing parameters from Pitzer:[6] $\theta_{K,H} = 0.005$, $\theta_{Cl,NO_3} = 0.016$, $\theta_{Na,H} = 0.036$, and $\theta_{Na,K} = -0.012$.

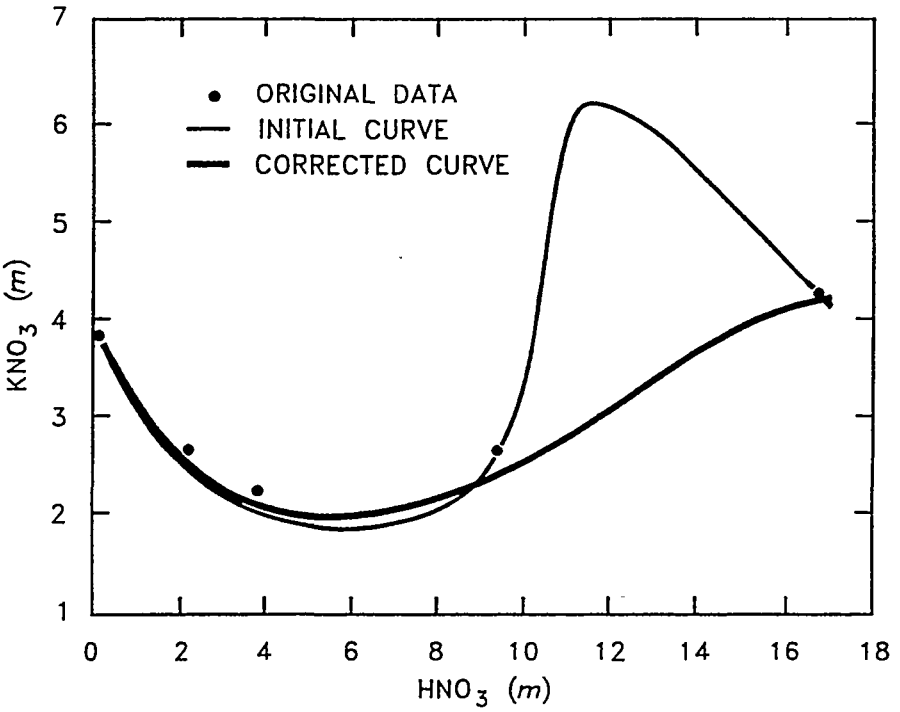

Fig. 6. Solubilities of KNO_3 in HNO_3 solution.

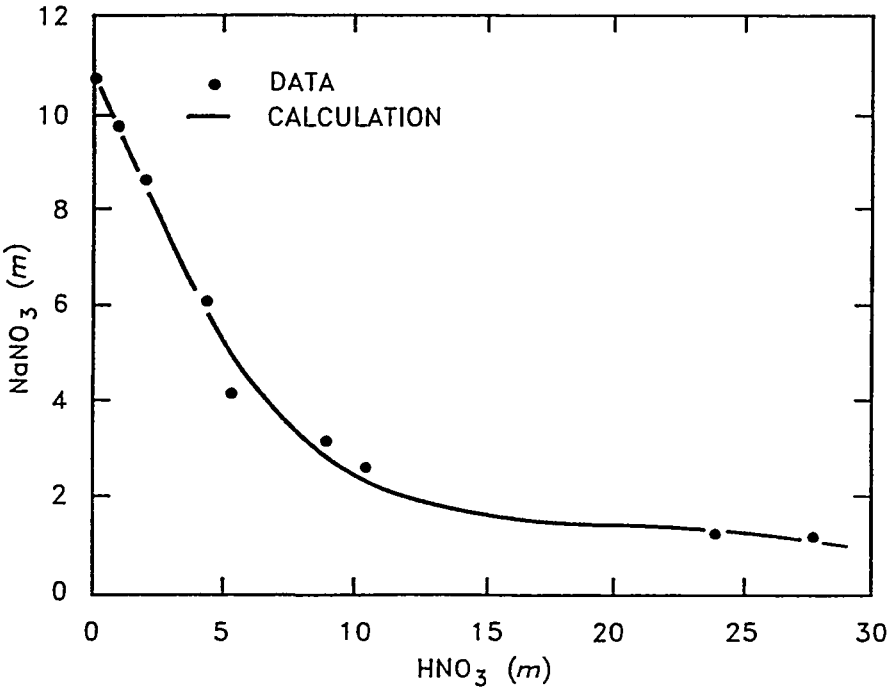

Fig. 7. Solubilities of $NaNO_3$ in HNO_3 solutions.

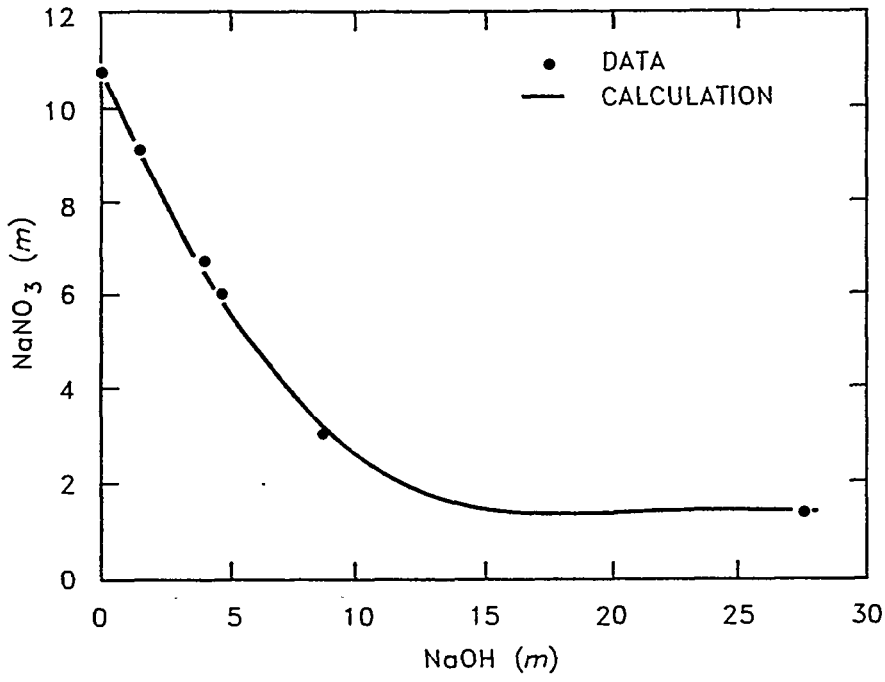

Fig. 8. Solubilities of $NaNO_3$ in NaOH solutions.

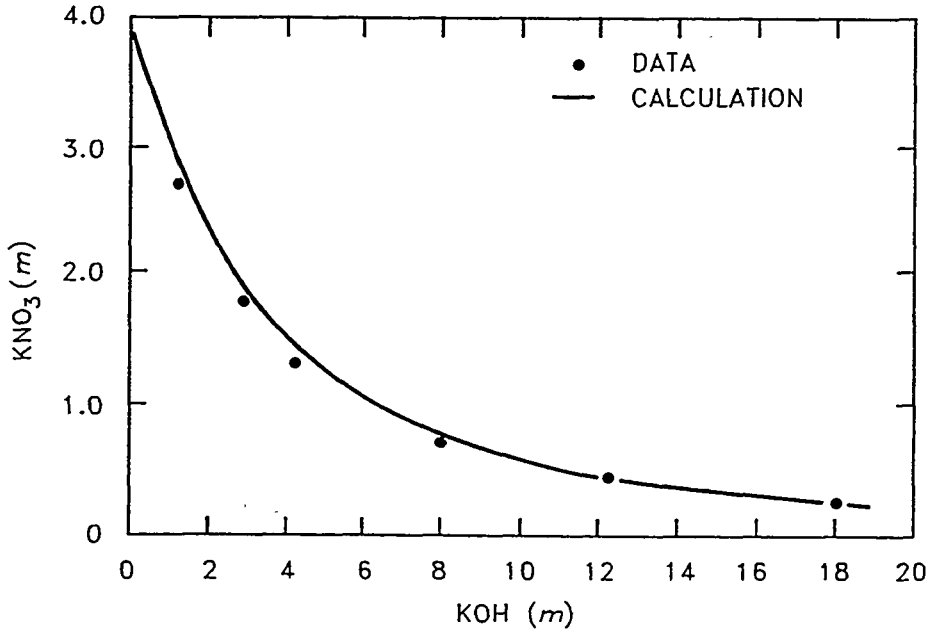

Fig. 9. Solubilities of KNO_3 in KOH solutions.

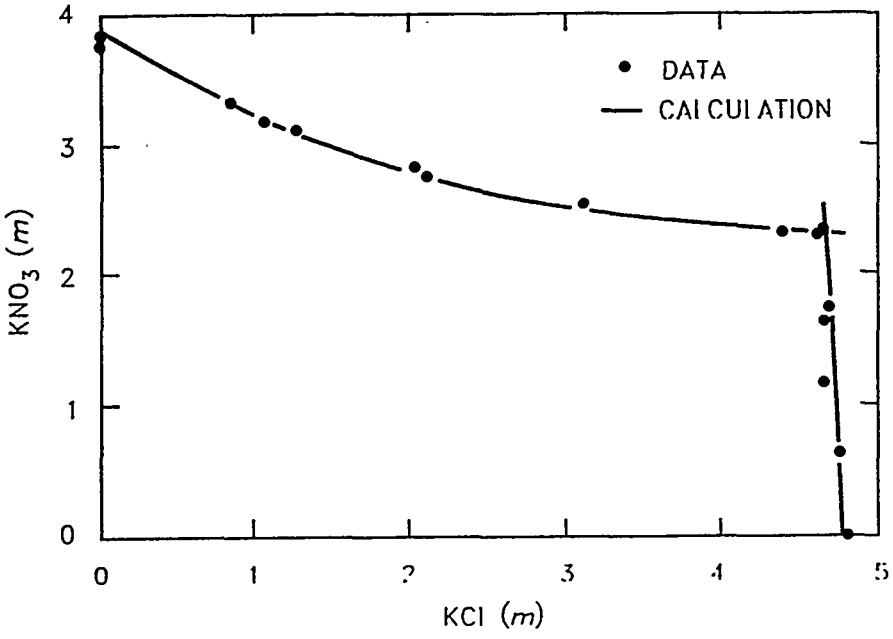

Fig. 10. Solubilities in the K-Cl-NO_3 system.

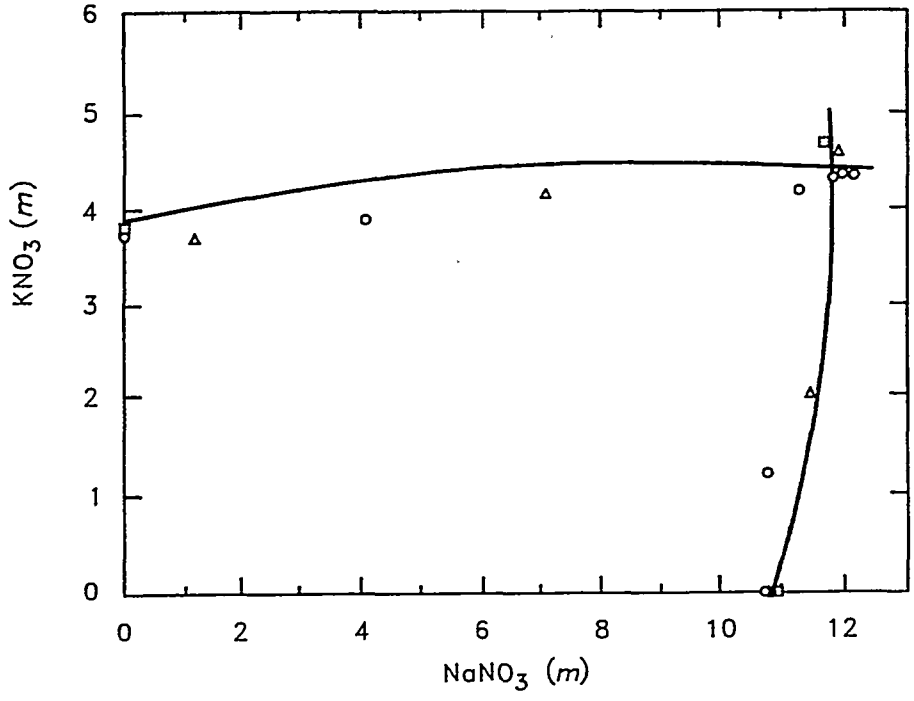

Fig. 11. Solubilities in the Na-K-NO_3 system. (o = data from ref. 18; Δ = data from ref. 19; and □ = data from ref. 28.)

Chemical potentials for the aqueous ions were obtained from the CODATA[15] evaluation (see Table 5). The chemical potentials for four solids are also shown, obtained by application of Eq. (17).

It was also expedient to represent activity coefficients using the Pitzer formulation at higher ionic strengths. The parameters for NaCl and $NaNO_3$ are already available[6] for $I \leq 6$, since these salts remain in solution and accurate data have been reported. For KNO_3, the parameter values obtained for data with $I \leq 3.5$ extrapolated very well to $I = 7$, producing nearly identical results with the expanded polynomial representations using the values in Table 4. For KCl, it was useful to revise the binary parameters to ensure accurate representation at ionic strengths above 4.8 (the solubility limit). This revision was done by a least-squares fit, using as data the predictions at many points obtained from Eqs. (2) and (4), and the parameters from Table 3. The optimal parameter values are given in Table 6, and the resulting activity coefficients are shown in Fig. 12. While the fit itself only encompassed the range $0.001 < I < 6$, the results provided excellent agreement to $I = 8$.

4.3 RESULTS FOR ASYMMETRIC MIXTURES: TERNARY SYSTEMS INVOLVING Ca^{2+}

We are principally concerned with mixtures of 1–1 electrolytes with 2–1, 1–2, or 2–2 electrolytes. Because of the presence of ions with different charge numbers, Eqs. (11) and (12) were no longer usable. Hence, the estimation of Pitzer mixing parameters could not involve Eqs. (2) and (4) for the binary solution and, therefore, would have to utilize the Pitzer binary formulas (9) and (10). This might present some difficulty if mixed solution data were used because the ionic strengths exceed the normal range of applicability for Pitzer binary parameters (usually $I \leq 6\ m$). In such cases, it might be possible to fit binary parameters to higher ionic strengths, although this would usually involve loss of accuracy at the lower values of ionic strength. In any event, binary parameters should be validated through the entire range of ionic strength required by the mixture data.

4.3.1 Ternary Systems Involving Ca^{2+}

We are primarily interested in the mixtures of $CaCl_2$ and $Ca(NO_3)_2$ with either K^+, Na^+, or H^+. Some data to be used involved higher ionic strengths (up to $I = 11.1$). For $CaCl_2$, a standard reference[6] lists values valid to $I = 13$ (see Table 7). For $Ca(NO_3)_2$, nonlinear fits to the data of Robinson and Stokes[16] with $3 \leq I \leq 12$ (i.e., $1 \leq m \leq 4$) yielded binary parameters (Table 7) that could be used in subsequent analyses. As was done for KCl in Sect. 4.2.4, binary Pitzer parameters for both KNO_3 and KCl were obtained by fitting to the extended polynomial forms [cf. Eqs. (2) and (4)], using coefficients in Tables 3 and 4; the resulting parameters and ranges of applicability are given in Table 7. Since NaCl and $NaNO_3$ will be needed up to $I = 8.5$, the binary parameters for these salts were also fit to the extended polynomial forms using coefficients in Tables 2 and 4. The results, given in Table 7, do not differ appreciably from the accepted values at lower ionic strengths.

The first row of Table 8 shows mixing parameters for the system K-Ca-Cl, as derived[6] from the isopiestic data of Robinson and Covington[17] up to $I = 5$. Using all the data of Robinson and Covington plus KCl solubility data in K-Ca-Cl solutions, together with the extended range binary

Table 5. Derived parameters

Species	μ^0/RT	Reference
$Na^+(aq)$	–105.695	15
$K^+(aq)$	–113.965	15
$NO_3^-(aq)$	–44.699	15
$Cl^-(aq)$	–52.928	15
NaCl(c)	–155.007	This work
KCl(c)	–164.878	This work
$NaNO_3(c)$	–147.803	This work
$KNO_3(c)$	–158.859	This work

Table 6. Binary Pitzer parameters at high ionic strengths

	Binary Pitzer parameters	Value	Range of fit	Range of applicability	Reference
KNO_3	β^0	–0.0816	$I \leq 3.5$	$I \leq 7$	6
	β^1	0.0494	$I \leq 3.5$	$I \leq 7$	6
	C^ϕ	0.0066	$I \leq 3.5$	$I \leq 7$	6
KCl	β^0	0.05957	$I \leq 6$	$I \leq 8$	This work
	β^1	0.1782	$I \leq 6$	$I \leq 8$	This work
	C^ϕ	–0.00433	$I \leq 6$	$I \leq 8$	This work

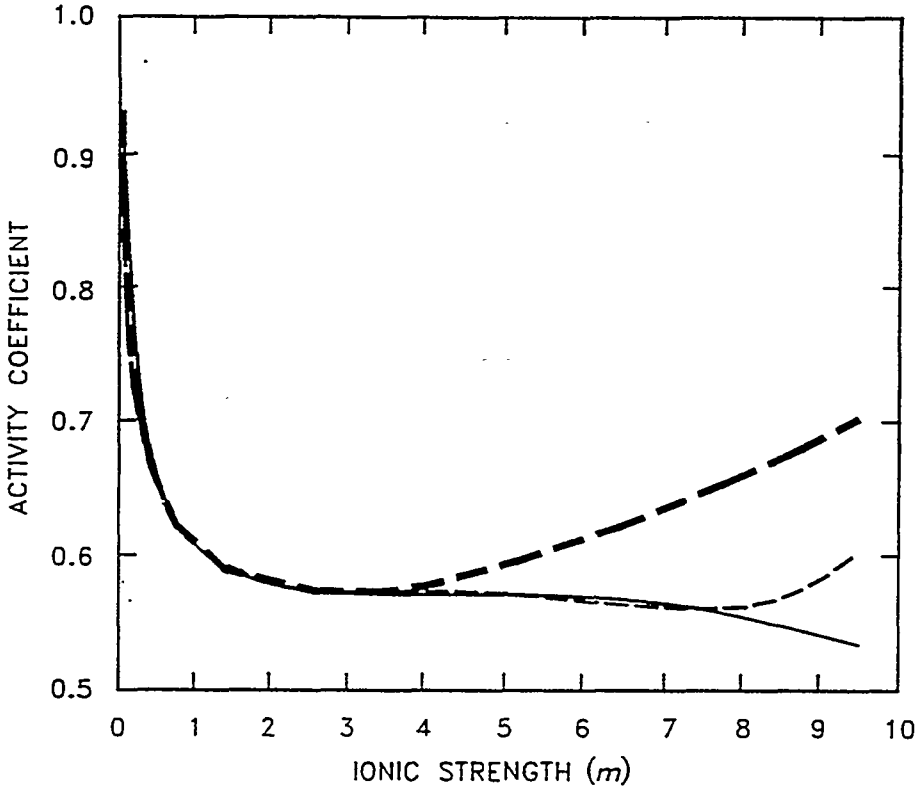

Fig. 12. Activity coefficients of KCl. Heavy broken line refers to Eq. (5) using parameters from ref. 6; light broken line refers to Eq. (5) using parameters in Table 6; solid line refers to Eq. (2).

Table 7. Binary parameters at extended ionic strengths

Solute	β°	β^1	C^ϕ	Range
$CaCl_2$[a]	0.3053	1.7085	0.00215	$I \le 12.9$
$Ca(NO_3)_2$[b]	0.1997	1.4320	–0.0153	$0.3 \le I \le 9$
	0.1839	1.5527	–0.0105	$3 \le I \le 12$
KCl	0.05957	0.1782	–0.00433	$0 \le I \le 8$
KNO_3	–0.09827	0.2118	0.00919	$3 \le I \le 11$
NaClO	0.06743	0.3301	0.00263	$0.5 \le I \le 8.5$
$NaNO_3$	-0.00055	0.2110	0.00082	$0.1 \le I \le 8.5$

[a]From ref. 6.
[b]From ref. 16.

Table 8. Mixing parameters for K-Ca-Cl and K-Ca-NO_3 systems

Case	Source	Parameter values			
		$\theta_{K\text{-}Ca}$	$\psi_{K\text{-}Ca\text{-}NO_3}$	$\psi_{K\text{-}Ca\text{-}Cl}$	$\mu^0_{KNO_3}/RT$
	a	0.032		–0.025	
	b,c	–0.1870		0.0242	
1	*b,c,d,e*	0.06144	–0.0209	–0.0225	–158.86
2	*b,c,d,e*	0.0337	–0.0178	–0.0173	–158.88
3	*b,c,d,e*	–0.01170	–0.0126	–0.0088	–158.91

[a]Reference 17; using only data with $I \leq 5$.
[b]Reference 17; isopiestic $0.9 \leq I \leq 6.3$.
[c]Reference 28; solubility data for KCl in CaCl solutions, four points, $4.8 \leq I \leq 8.4$.
[d]Reference 19; solubility data for KNO_3 in $Ca(NO_3)_2$, six points $3.7 \leq I \leq 11.1$.
[e]Reference 18; excluding four points with Ca^{2+} between 0.1 and 1.2 *m*.

parameters in Table 7, yielded the values shown in the second row of Table 8. These two sets of mixing parameters exhibited marked differences; hence, additional evaluation was warranted. Furthermore, it was appropriate to consider additional systems in determining the cation interaction parameter $\theta_{K,Ca}$.

Only solubility data are available for obtaining mixing parameters in the K-Ca-NO_3 system. The values of Hamid and Ram Das[18] are older and more suspect. The data of Flatt and Bocherens[19] are somewhat more consistent with recent Russian measurements,[20] as shown in Fig. 13. In the range of $Ca^{2+} \leq 3$ *m*, they also correspond closely with the phase diagram given by Bergman and Opredelenkova.[21] We are concerned only with the region for which $Ca(NO_3)_2 \leq 2.5$ *m*, where KNO_3 is the precipitating species and $I \leq 11.1$. In this region, the two data sets demonstrate considerable disparity, which presents high uncertainty for the calculation of mixing parameters. Numerous approaches were used, including (1) variation of the chemical potential for KNO_3 from the nominal value in Table 5, (2) inclusion of the K-Ca-Cl data and simultaneous optimization of mixing terms in both chloride and nitrate systems, and (3) omission of some of the data of Hamid and Ram Das[18] as outliers. The best approach must be assessed somewhat heuristically, which is the inevitable result of poor data.

Three particular results are listed in Table 8 and plotted in Figs. 14–18. The following observations of these cases can be made:

1. All three results do a credible job of approximating the K-Ca-Cl isopiestic data of Robinson and Covington. Case 3 is the best, and case 1 is the worst. Case 2, which is nearly as good as Case 3, is illustrated in Fig. 14.

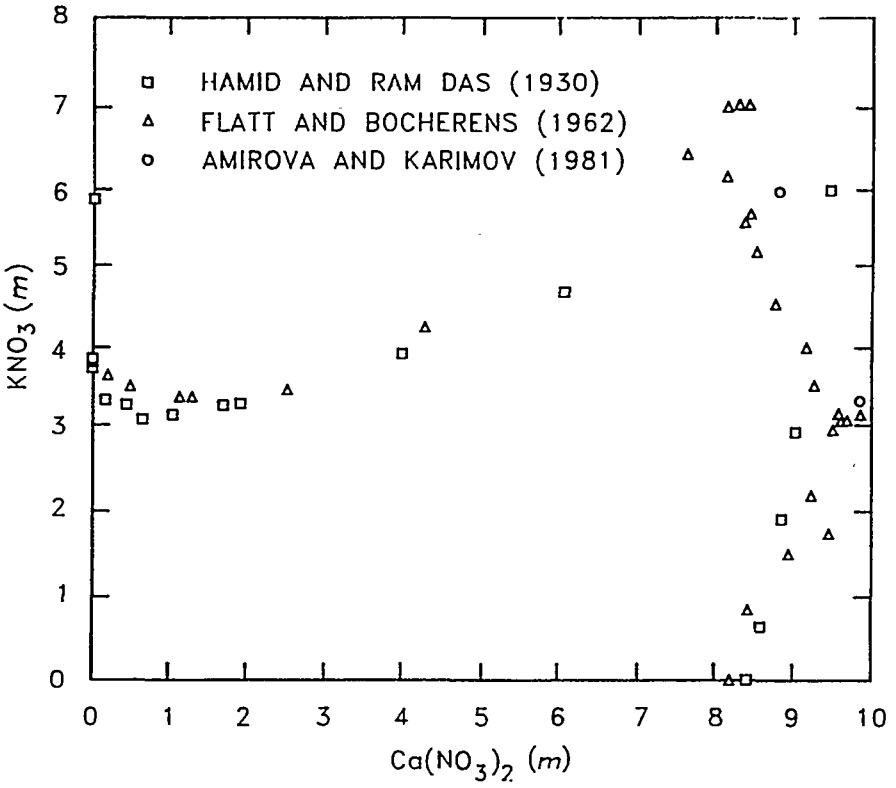

Fig. 13. Complete solubility diagram of K-Ca-NO_3 system at 25°C.

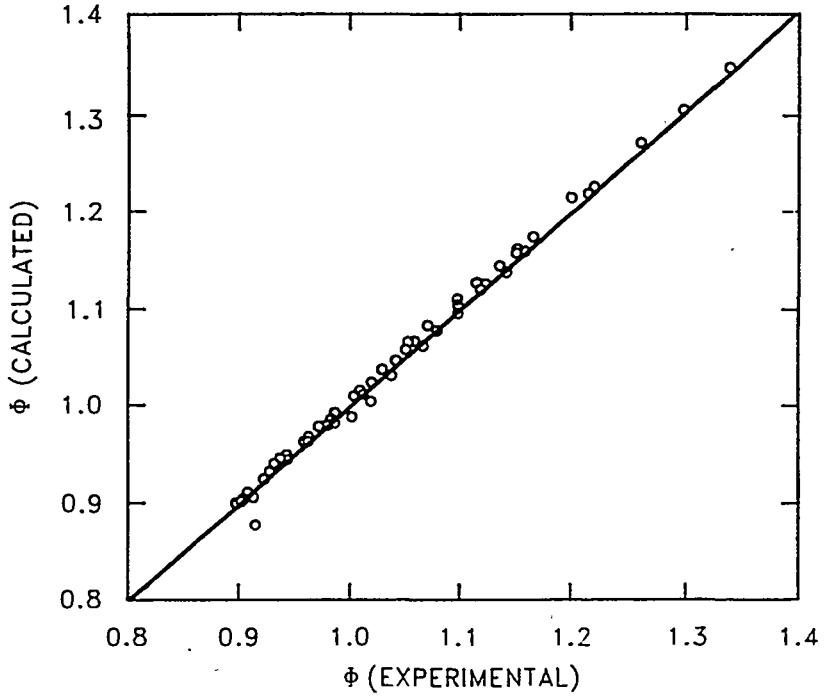

Fig. 14. Osmotic coefficients for K-Ca-Cl system.

2. All three results provide excellent calculations of KCl solubilities, as shown in Fig. 15. They are so close that it is difficult to distinguish the individual plot lines.

3. The optimal least-squares solution for all data is the last one ($\mu^0_{KNO_3} = -158.910$); the sum of squared error (SSE) rises as $\mu^0_{KNO_3}$ increases from this value, as shown in Fig. 16.

4. The value of $\theta_{K,Ca}$ is highly sensitive to changes in the free energy of formation $\mu^0_{KNO_3}$. The mixing parameters ψ_{K,Ca,NO_3} and $\psi_{K,Ca,Cl}$ are much less sensitive, as illustrated in Fig. 17.

5. The last two cases provide reasonably good fits to the KNO_3 solubilities in $Ca(NO_3)_2$ solutions, as shown in Fig. 18, while the first case models this system only marginally.

We consider case 1 only because the value of $\mu^0_{KNO_3}$ is that of Table 5, which reflects the parameter fits in Sect. 4.2.3 involving KNO_3 in HNO_3, KOH, and KCl solutions. However, in the present circumstances, this value for $\mu^0_{KNO_3}$ is clearly inferior. The optimal least-squares solution is case 3, which represents all the data quite nicely; however, the value for $\mu^0_{KNO_3}$ deviates somewhat from the earlier value in Table 5. Finally, case 2 has a value of $\mu^0_{KNO_3}$ that is fairly close to that in Table 5 and an SSE not much greater than that of case 3; it also represents the data well, as depicted in Figs. 14, 15, and 18. Case 2 has the added advantage that the values of the mixing parameters $\theta_{K,Ca}$ and $\psi_{K,Ca,Cl}$ are very close to previous values (in the first row of Table 8).

With regard to systems Na-Ca-Cl and Na-Ca-NO_3, evaluations of parameters have been done by Pitzer[22] and Smith et al,[23] respectively, whose results are shown in Table 9. Because of the disparity in the $\theta_{Na,Ca}$ term, reevaluation is necessary. By using two sets of data[23-25] for each system, a simultaneous fitting of all mixing parameters yielded the results in the last line of Table 9. (Note: The binary system values in Table 6 were used.) These values characterize the two systems quite well, as shown in Figs. 19–21.

The evaluation of interaction parameters in mixed solutions involving H^+ and Ca^{2+} has involved only halide anions. Two studies produced the results shown in Table 10. Harvie and Weare used the emf data of Roy et al[26] and solubility data for H-Ca-Cl systems. Their results involved more than one anion, their value of $\theta_{H,Ca}$ is preferred, although it made no difference in our calculations which value was used.

The single mixing parameter ψ_{H,Ca,NO_3} was estimated using the KNO_3 solubility data of Flatt and Bocherens[27] for the K-Ca-H-NO_3 system. Other required mixing parameters are found in Tables 3 and 8. As mentioned, either value in Table 10 for $\theta_{H,Ca}$ produced the same results; however, considerable variation in ψ occurred with small changes in $\mu^0_{KNO_3}$. The three cases in Table 8 were also used here, producing the results shown in Table 10. Again, case 3 yields the least-squares optimal result, case 2 is close, and case 1 is somewhat higher. A comparison of the calculated and experimental solubilities is shown in Fig. 22. Both cases 2 and 3 give good results, whereas those from case 1 are not as satisfactory.

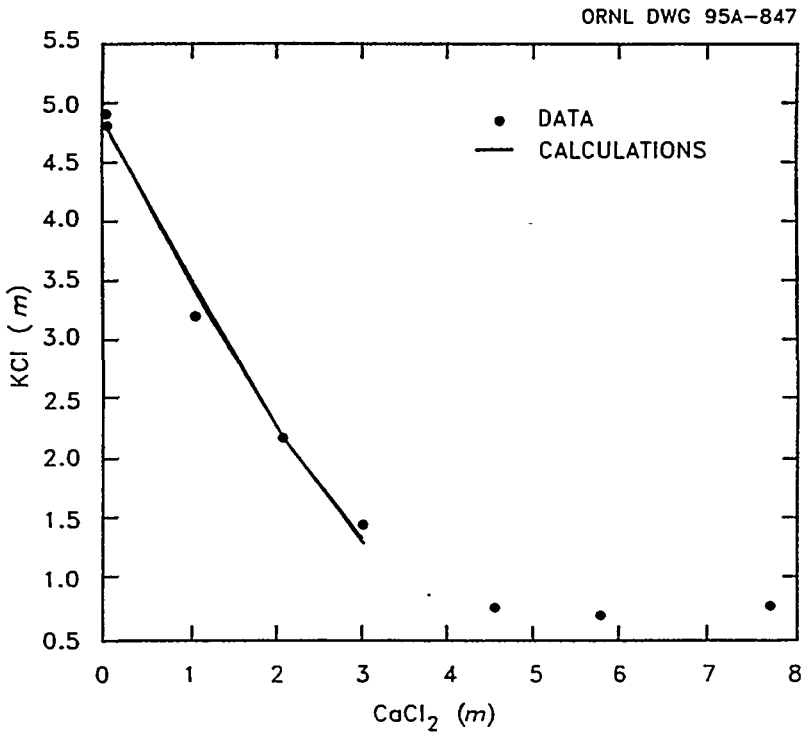

Fig. 15. Solubility of KCl in $CaCl_2$ solutions.

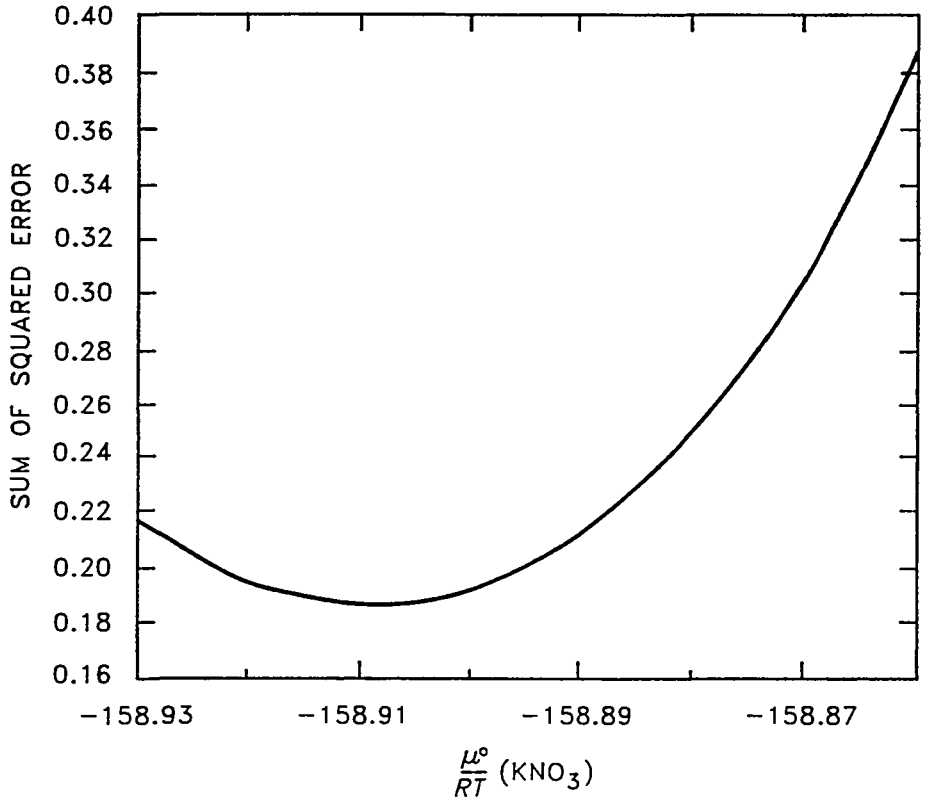

Fig. 16. Optimization of K-Ca mixing parameters.

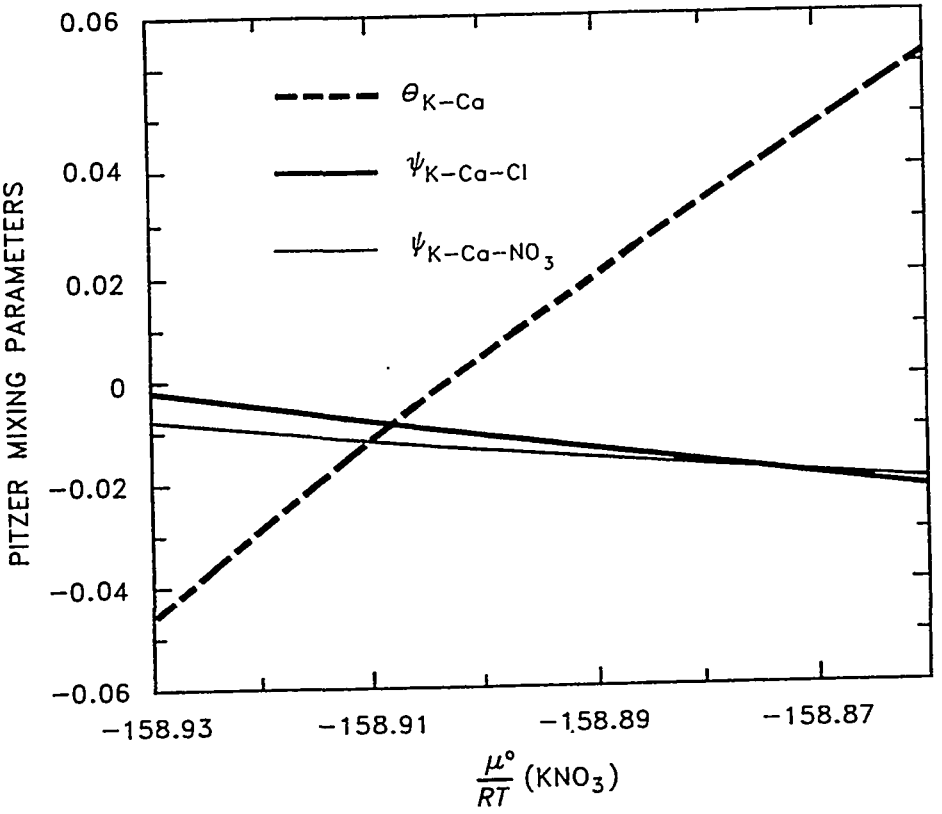

Fig. 17. Variation of mixing parameters in K-Ca systems.

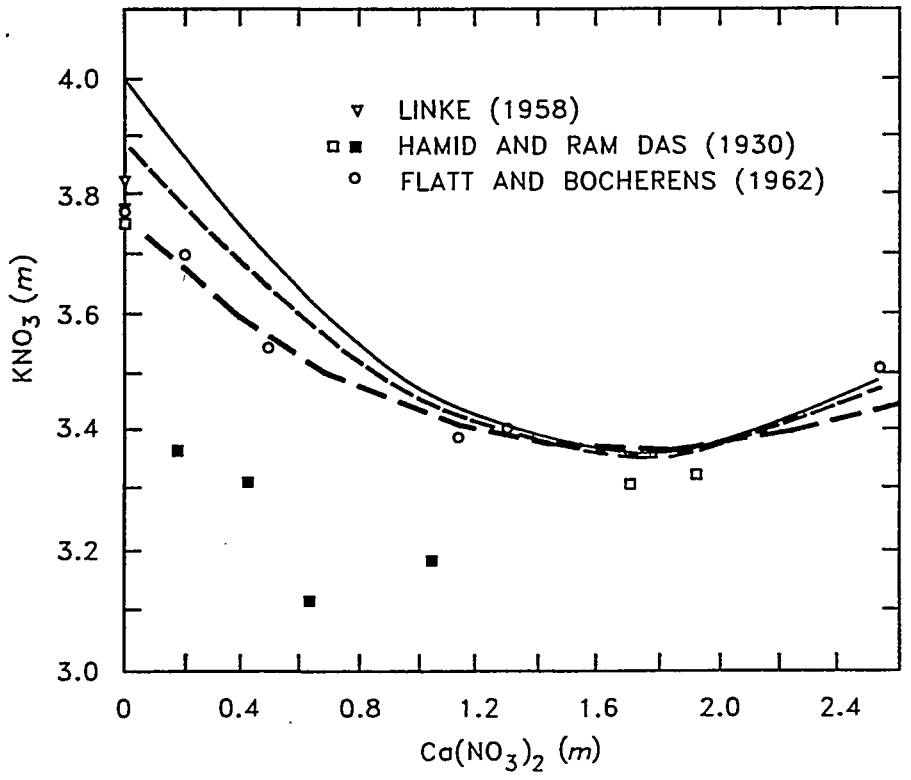

Fig. 18. Solubility of KNO_3 in $Ca(NO_3)_2$ solutions. Solid line refers to calculations using case 1; broken line refers to case 2; and dotted line refers to case 3 from Table 8.

Table 9. Mixing parameters for Na-Ca-Cl and Na-Ca-NO_3 systems

Parameter values			Reference	
$\theta_{Na,Ca}$	$\psi_{Na,Ca,Cl}$	$\psi_{Na,Ca,NO3}$	Parameter	Data
0.070	–0.007	–	22	*a*
–0.2411	–	0.07985	23	*b*
0.0975	–0.0100	–0.0174	This work	*a,b,c*

[a]Reference 24; isopiestic data for Na-Ca-Cl (53 points, $0.7 \le I \le 8$).
[b]Reference 23; emf data for Na-Ca-NO_3 (96 points, $0.1 \le I \le 2$).
[c]Reference 25; isopiestic data for both Na-Ca-Cl (40 points, $3.6 \le I \le 8.6$) and Na-Ca-NO_3 (45 points, $3.7 \le I \le 8.7$).

Table 10. Mixing parameters for H-Ca systems

Parameter values				
$\theta_{H,Ca}$	$\psi_{H,Ca,Cl}$	$\psi_{H,Ca,Br}$	$\psi_{H,Ca,NO3}$	Reference
0.092	–0.15			12
0.0682	0.0043	0.0285		9
(0.0682)[a,b]			0.0169	This work; $\mu^0_{KNO_3}/RT = -158.86$
(0.0682)			0.0082	This work; $\mu^0_{KNO_3}/RT = -158.88$
(0.0682)			–0.0044	This work; $\mu^0_{KNO_3}/RT = -158.91$

[a]Quantities in parentheses were not optimized.
[b]This value could vary substantially without changing the value of $\psi_{H\text{-}Ca\text{-}NO_3}$.

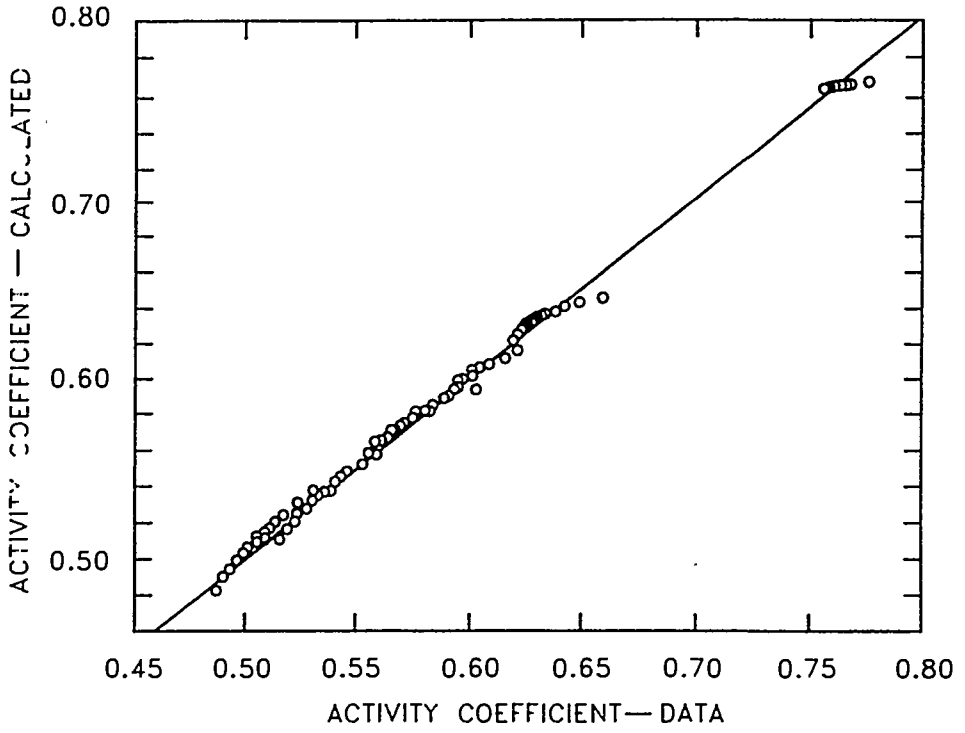

Fig. 19. Calculated vs experimental activity coefficients for Na-Ca-NO_3 system.

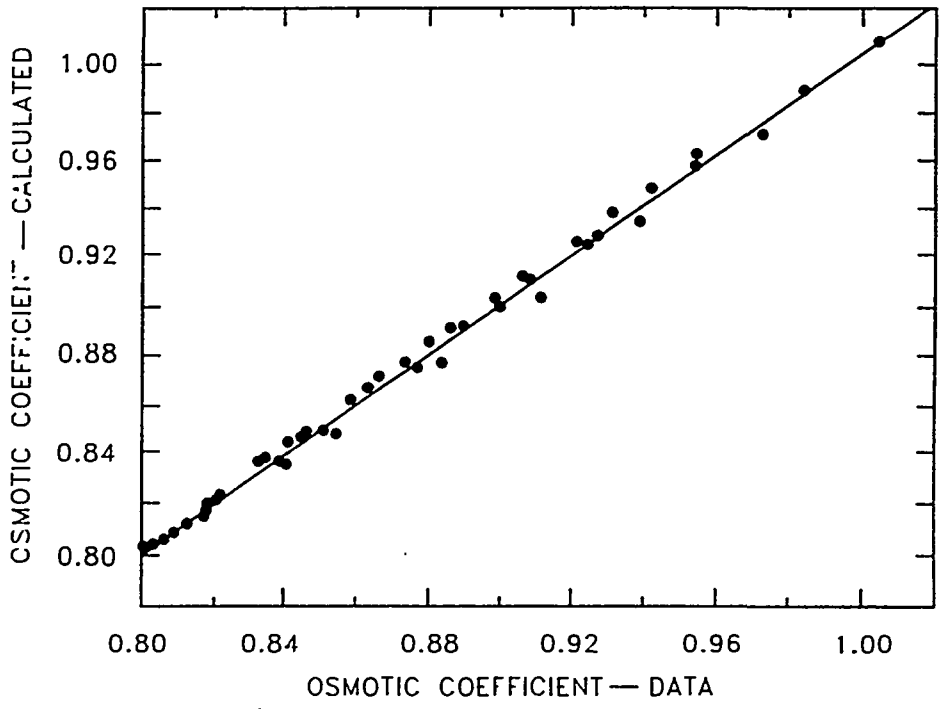

Fig. 20. Calculated vs experimental osmotic coefficients for the Na-Ca-NO_3 system.

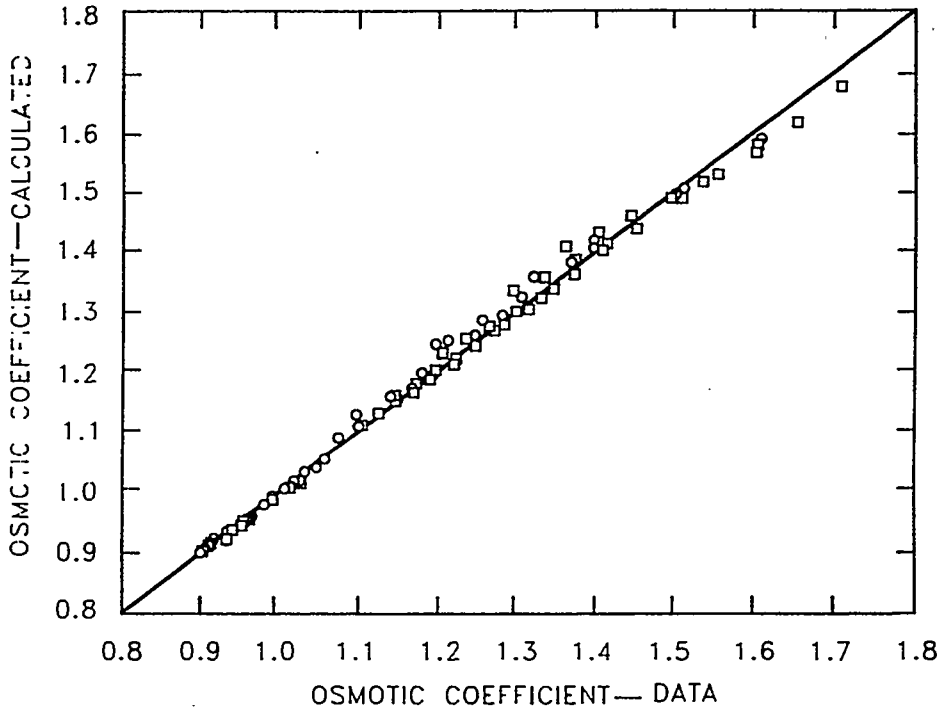

Fig. 21. Calculated vs experimental osmotic coefficients for the Na-Ca-Cl system. o = data from ref. 24; □ = data from ref. 25.

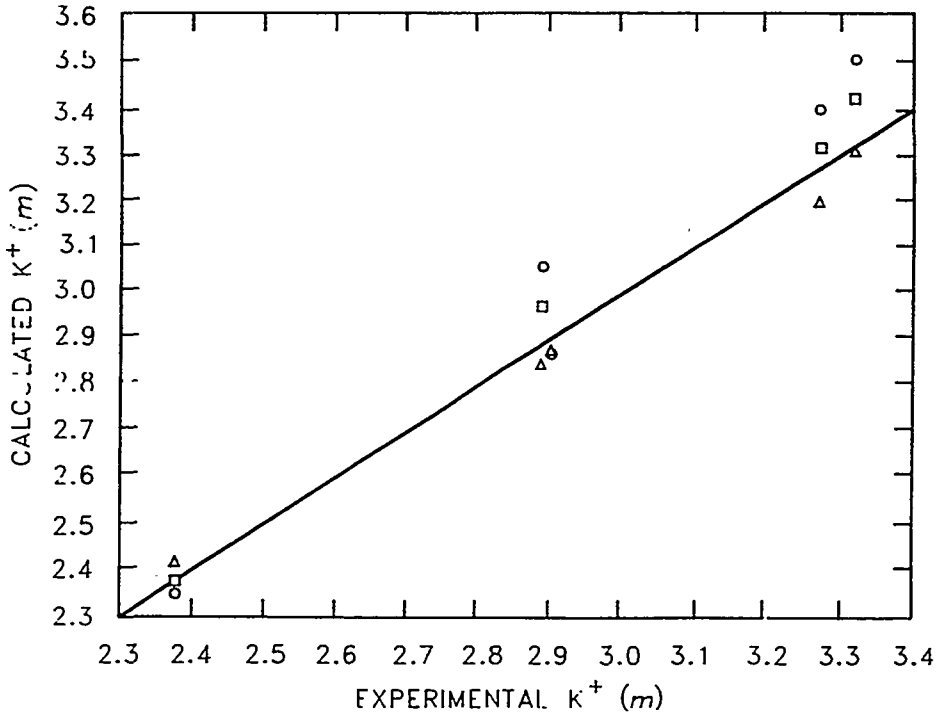

Fig. 22. Solubilities of KNO_3 in the K-H-Ca-NO_3 system.

4.4 SYSTEMS INVOLVING $Ca(OH)_2$

Using the results of previous sections, we are now in a position to consider the behavior of $Ca(OH)_2$. For this substance, we need not only the mixture parameters ψ, but the binary Pitzer parameters as well. The low solubility prevents us from obtaining these values simply by measuring activity and osmotic coefficients to high molalities. However, in our analysis, we could estimate binary and mixture parameters simultaneously, using solubility data for a number of salt systems. While we often consult the original sources of data, a primary reference for solubility data is the compendium by Linke.[28]

Harvie et al.[12] used emf measurements in KCl and $CaCl_2$ solutions, together with solubility data in CaCl to obtain binary parameters for $Ca(OH)_2$, as shown in Table 11. However, their results would contain an inherent bias for chloride systems. In addition, they involved ionic strengths that exceeded the valid range for other binary parameters. Thus, it is questionable whether such results would be applicable to systems with high concentrations of NO_3^-, OH^-, and anions other than Cl^-.

We used the emf data of Bates et al.[29] and solubility data from a variety of salt systems, as listed in Table 12. The combined data sets contained 111 data points. Each solubility point had a weight of unity, whereas the emf data were represented by 0.01 ln ($a_H a_{Cl^-}$) (i.e., the logarithm of the activity product, weighted by 0.01). Initially, these data were used to estimate 8 parameters: the three binary parameters β^0, β^1, and C; the free energy, μ^0, for $Ca(OH)_2$; and the mixture parameters $\psi_{Ca,OH,\alpha}$, where $\alpha = NO_3^-$, Cl^-, Na^+, and K^+.

Attempts to implement the optimization scheme revealed a parametric redundancy that inhibited the actual mathematical optimization procedure. Such problems arise from 3 sources: (1) ineffective parameter normalization (i.e., parameters having widely varying nominal values and sensitivities), (2) imprecision in the data, which prevents determination of the effects of similar parameters, and (3) model formulation using dependent parameters. To permit all three types of problems to be handled simultaneously, the values of C and μ^0 were fixed and the remaining parameters optimized. The global optimum could be realized by using a number of trial values for C and μ^0 . With each choice of fixed parameters, the mathematical procedure converged independently of the initial guess.

Results of this optimization are shown on the third row of Table 11. The optimal value of μ^0 was independent of C or any of the other parameters; however, all other parameters exhibited considerable dependence on each other, especially on the choice of C. Furthermore, the sum of SSE was largely independent of C, indicating that the above-mentioned problems (2) or (3) might be significant. Hence, C was arbitrarily set to zero because the data were insufficient (due either to imprecision or model formulation) to estimate it simultaneously with the mixture parameters. Furthermore, the model is still widely applicable since any interactions of Ca-OH at high ionic strength will necessarily involve some additional ion.

A second optimization was performed in which the additional binary parameter β^2 was considered and the quantities B and B^0 were replaced in Eqs. (5) and (6) with

$$B^{\phi} = \beta^0 + \beta^1 e^{-\alpha_1\sqrt{I}} + \beta^2 e^{-\alpha_2\sqrt{I}}$$

and

Table 11. Pitzer parameters for $Ca(OH)_2$ systems

μ^0/RT	β^0	β^1	β^2	C^ϕ	ψ_{Ca,OH,NO_3}	$\psi_{Ca,OH,Cl}$	$\psi_{Na,Ca,OH}$	$\psi_{K,Ca,OH}$	Reference
–362.67									15
–362.12	–0.1747	–0.2303	–5.72			–0.025			12
–361.869	0.1255	–1.9844		0	–0.0466	–0.1195	–0.0431	–0.0505	This study
–361.819	–0.2169	0.06968	–9.372		0.0577	–0.0165	–0.0270	0.0027	This study

Table 12. Data for estimation of $Ca(OH)_2$ parameters

Type	Salt medium	Maximum ionic strength	No. of points	Reference
Solubility	NaCl	3.8	12	30
Solubility	KCl	3.0	10	30
Solubility	$NaNO_3$	4.8	11	30
Solubility	$NaNO_3$	4.8	7	31
Solubility	$Ca(NO_3)_2$	5.4	7	32
Solubility	$Ca(NO_3)_2$	6.1	7	33
Solubility	$CaCl_2$	6.1	7	28
Solubility	$CaCl_2$	6.3	6	34
Solubility	NaOH	0.51	7	35
Solubility	NaOH	0.21	6	36
Solubility	KOH	0.22	7	36
emf	KCl	0.082	18	29
emf	$CaCl_2$	0.078	8	29

$$B = \beta^0 + \beta^1 g(\alpha_1\sqrt{I}) + \beta^2 g(\alpha_2\sqrt{I}),$$

where the function $g(x)$ was defined previously [following Eq. (6)], $\alpha_1 = 1.4$, and $\alpha_2 = 12$.

Using the optimal parameter values from Table 11, each of the salt systems can be simulated. Calculated values for the two parameter sets obtained in this work were nearly identical except for the solubility data in $Ca(NO_3)_2$ and $CaCl_2$ and the emf measurements. All results, shown in Figs. 23–31, generally show quite good agreement with the data. Probably the worst case is that for solubility data in NaCl, where computed values are about 10% low at the higher ionic strengths.

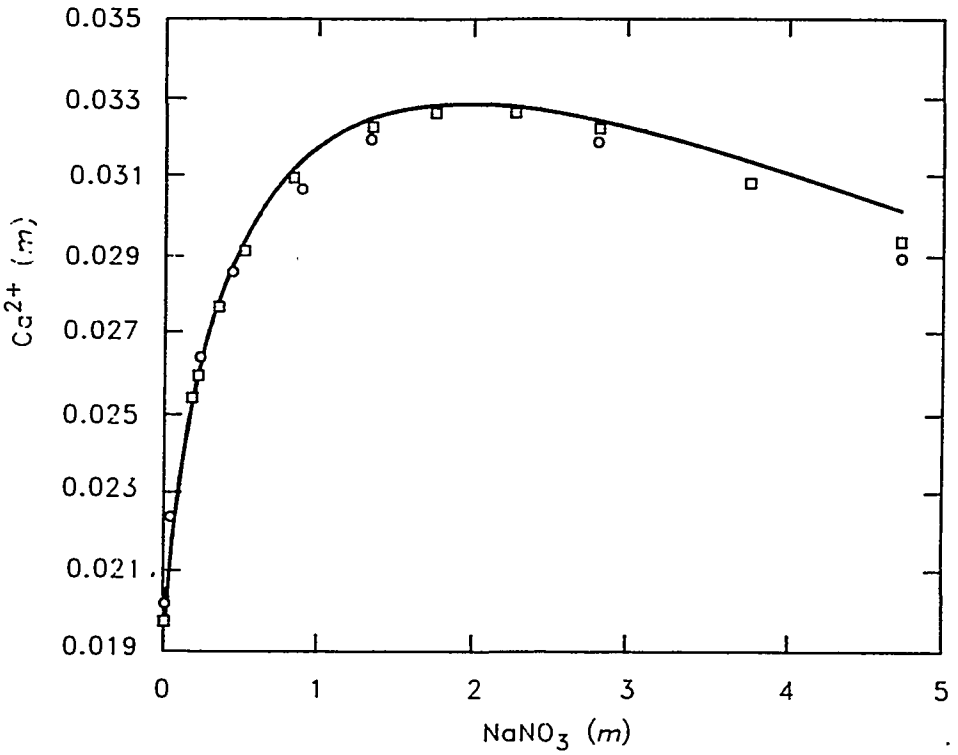

Fig. 23. Solubilities of $Ca(OH)_2$ in $NaNO_3$ solutions. □ = data from ref. 30; o = data from ref. 31.

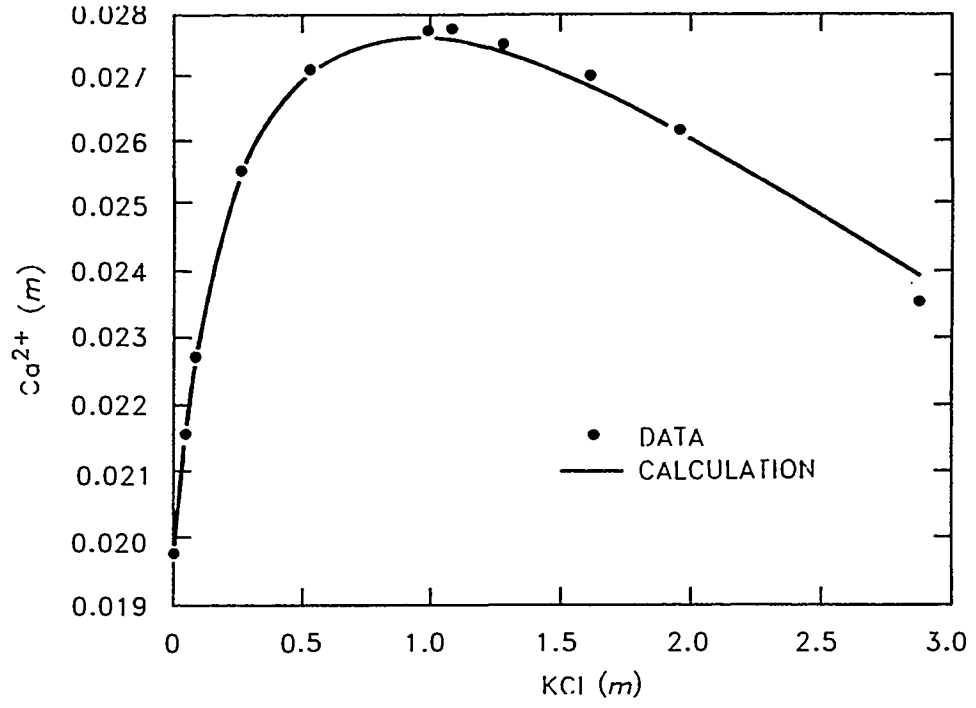

Fig. 24. Solubilities of $Ca(OH)_2$ in KCl solutions.

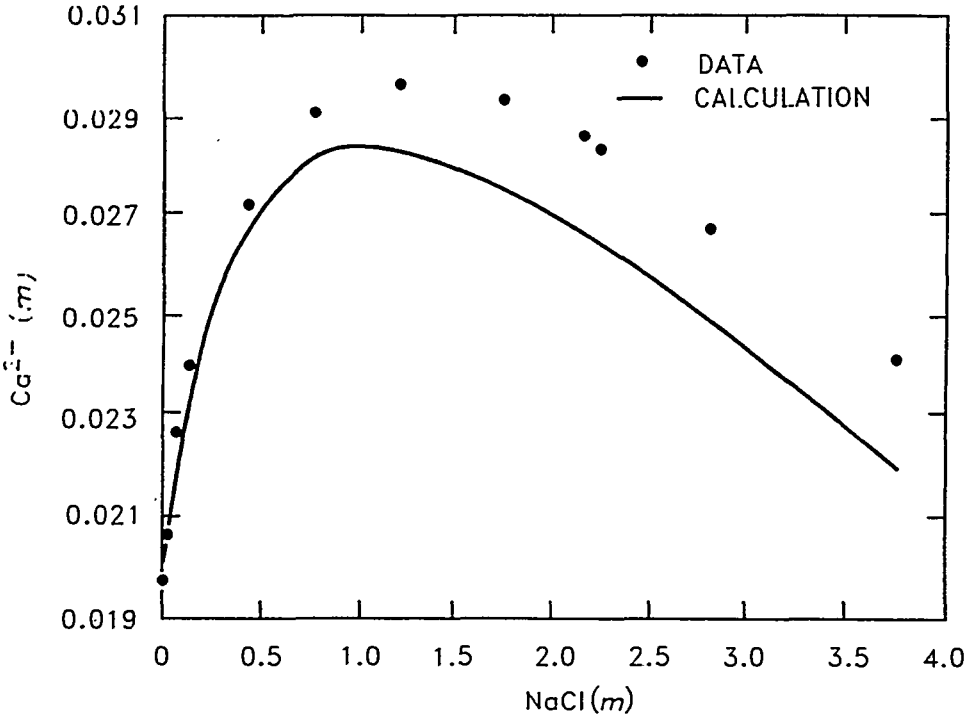

Fig. 25. Solubilities of $Ca(OH)_2$ ini NaCl solutions.

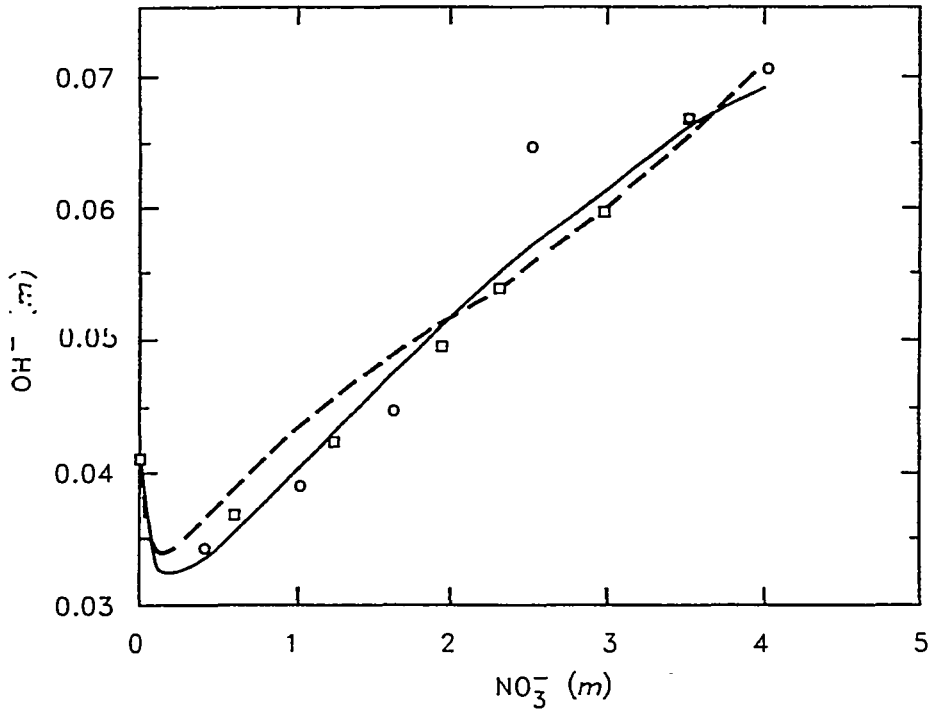

Fig. 26. Solubilities of $Ca(OH)_2$ in $Ca(NO_3)_2$ solutions. □ = data from ref. 32; o = data from ref. 33. Broken line refers to calculations using $\beta^2 = 0$; solid line refers to calculations using $\beta^2 = -9.372$; other respective parameters are shown in Table 11.

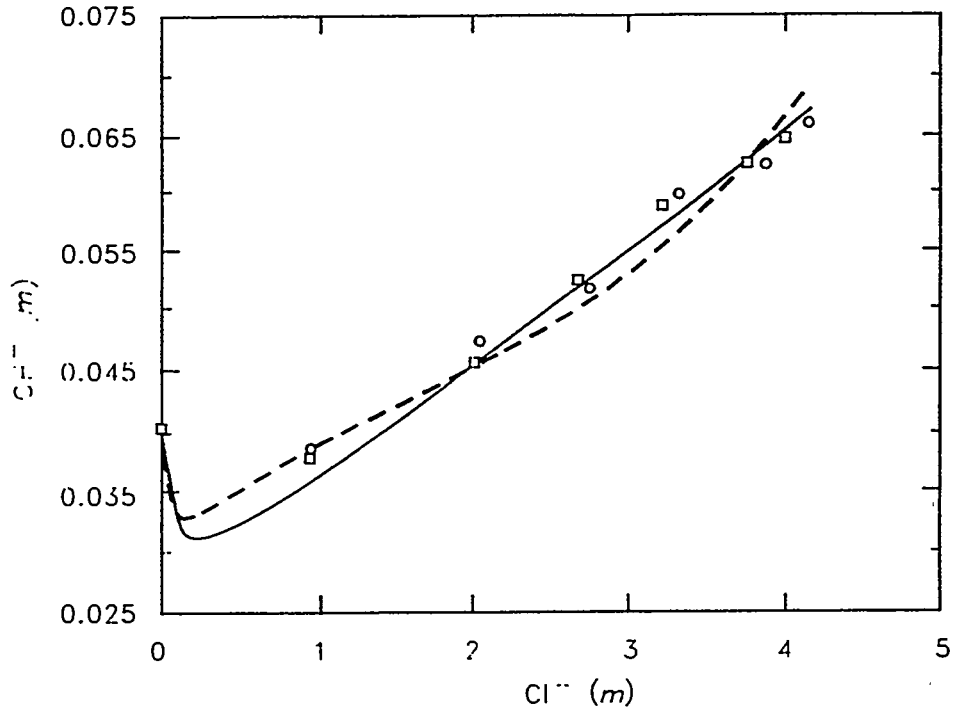

Fig. 27. Solubilities of $Ca(OH)_2$ in $CaCl_2$ solutions. □ = data from ref. 28; o = data from ref. 34. Broken line refers to calculations using $\beta^2 = 0$; solid line refers to calculations using $\beta^2 = -9.372$; other respective parameters are shown in Table 11.

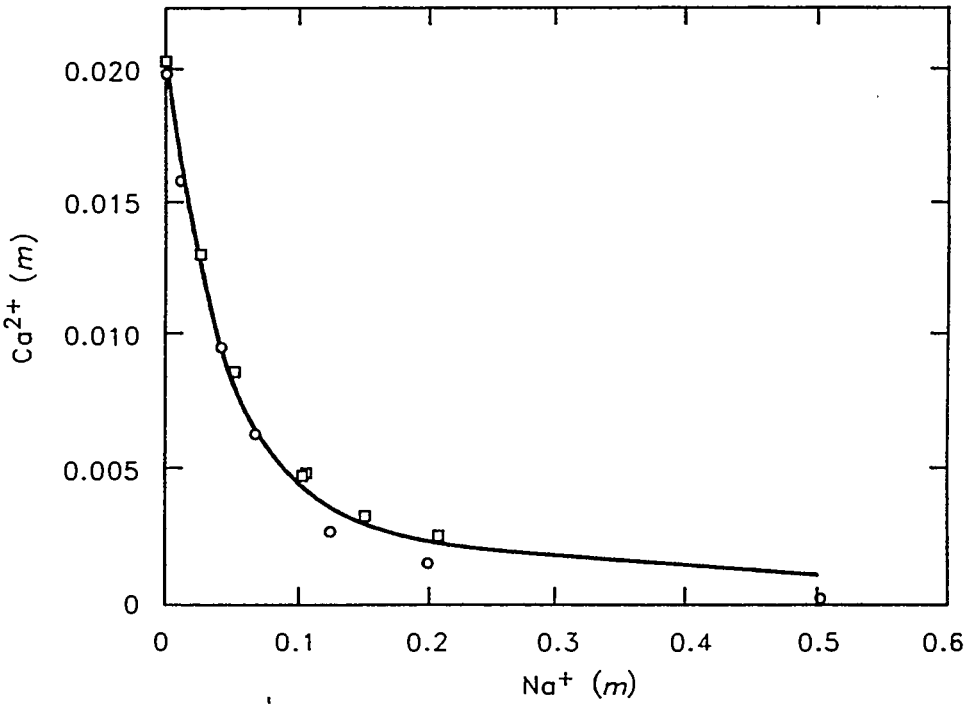

Fig. 28. Solubilities of $Ca(OH)_2$ in NaOH solutions. o = data from ref. 35; □ = data from ref. 36.

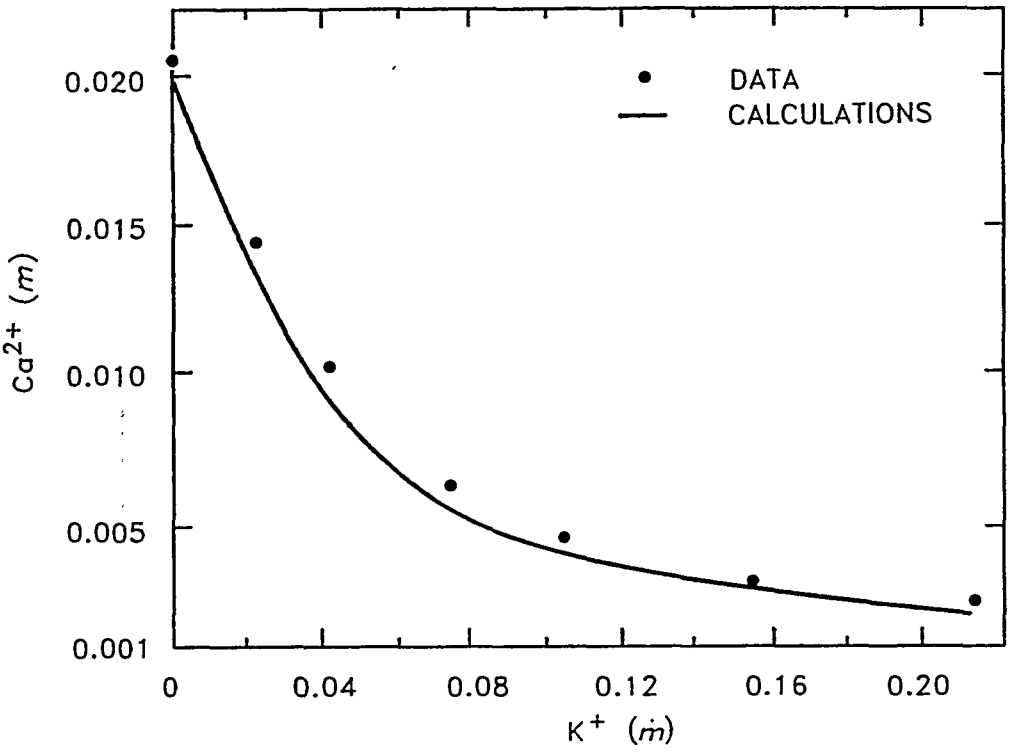

Fig. 29. Solubilities of $Ca(OH)_2$ in KOH solutions.

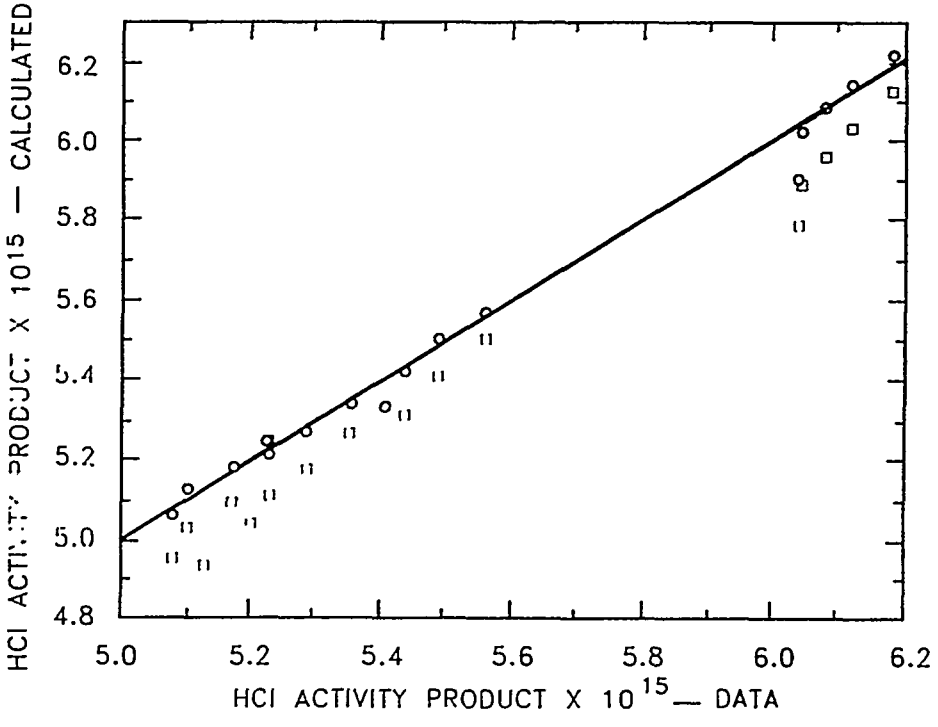

Fig. 30. Solubilities of $Ca(OH)_2$ in KCl solutions—emf measurements of HCl activity product. □ = calculations using $\beta^2 = 0$; o = calculations using $\beta^2 = -9.372$; other respective parameters shown in Table 11.

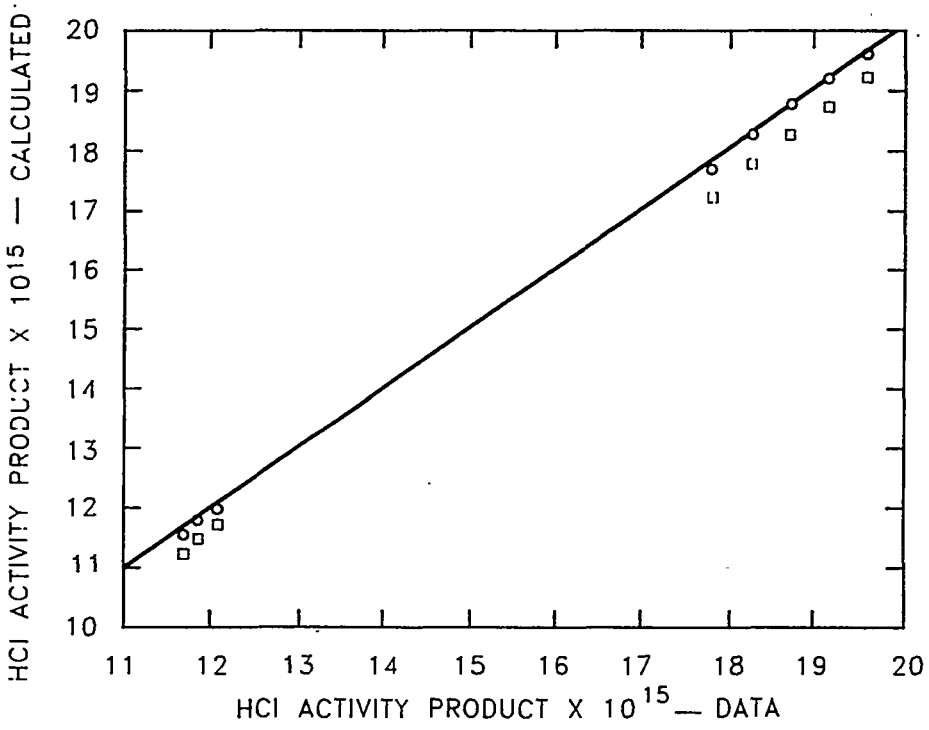

Fig. 31. Solubilities of $Ca(OH)_2$ in $CaCl_2$ solutions—emf measurements of HCl activity product. □ = calculations using $\beta^2 = 0$; o = calculations using $\beta^2 = -9.372$; other respective parameters shown in Table 11.

5. APPLICATION TO MIXED-WASTE SLUDGES

The parameters estimated in the previous section were combined with the existing Pitzer parameters and free energies of formation to yield a data base for the thermodynamic modeling of low-level waste sludges. The species included and parameter values used are tabulated in Appendix A. Of course, there are still many ion interactions that are poorly characterized (i.e., there is an incomplete set of parameters), and several of the free energies are not well known. Nevertheless, the available data are sufficient for scoping calculations.

These parameters can be used to calculate the chemical equilibrium for any system, given the inventories of elements. For most applications, phase equilibria are obtained using a modified form of the SOLGASMIX code. Certain calculations are occasionally checked against other calculational software to ensure the integrity of the computations.

This model (i.e., the parameters in Appendix A, coupled with the equilibrium calculation) was used to evaluate an actual sludge sample from MVST-25 at ORNL. Inventories of all principal components and several important trace elements were measured (see Table 13). With these inventories, the thermodynamic model could be used to estimate the species actually present, as shown in Table 14. In addition to the analytical data, the amount of CO_3^{2-} in the supernatant was

Table 13. Inventories of selected primary constituents from MVST-25 sludge (per kg of sludge)

Component	Supernatant[a] (g)	Dry solids[b] (g)	Total in sludge (g)	Total in sludge (mol)
Al	0.1685	8.385	8.554	0.31701
Ca	0.0035	31.232	31.236	0.77934
Co		0.013	0.013	0.00022
Fe		2.795	2.795	0.05005
K	5.208	4.680	9.888	0.25290
Mg		4.388	4.388	0.18052
Na	33.108	35.750	68.858	2.99515
Si		4.973	4.973	0.17705
Sr	0.000148	0.182	0.182	0.00208
U	0.0016	8.970	8.972	0.03770
Br^-	0.1283	0.227	0.356	0.00445
Cl^-	1.3913	1.203	2.594	0.07316
F^-	0.1380	0.617	0.756	0.03977
CO_3^{2-}	5.8426	37.375	43.218	0.72018
NO_3^-	87.792	58.175	145.967	2.35412
PO_4^{3-}		9.588	9.588	0.10095
SO_4^{2-}	0.8816	2.275	3.157	0.03286

[a]Values taken from ref. 37.
[b]Values taken from ref. 38.

Table 14. Distribution of species at equilibrium[a]

Species	Moles	Activity	Molality
Aqueous phase			
H_2O	3.3456E+01	8.6880E-01	5.5509E+01
Na^+	2.8061E+00	2.1045E+00	4.6557E+00
K^+	2.5290E-01	1.0607E-01	4.1960E-01
Ca^{2+}	3.4929E-06	3.1875E-07	5.7952E-06
Mg^{2+}	2.0549E-10	1.4133E-10	3.4093E-10
Sr^{2+}	1.6892E-05	8.6905E-07	2.8026E-05
Co^{2+}	8.5361E-14	2.1432E-14	1.4163E-13
H^+	1.9163E-14	3.8752E-14	3.1794E-14
NO_3^-	2.3210E+00	1.2252E+00	3.8509E+00
Cl^-	1.1738E-01	1.5183E-01	1.9475E-01
CO_3^{2-}	1.6428E-01	1.0513E-02	2.7256E-01
HCO_3^-	1.3473E-05	8.4975E-06	2.2354E-05
$Al(OH)_4^-$	2.3126E-02	2.1905E-02	3.8369E-02
OH^-	2.0045E-01	2.2112E-01	3.3257E-01
PO_4^{3-}	9.2464E-04	1.5341E-06	1.5341E-03
HPO_4^{2-}	4.7318E-06	1.3923E-07	7.8507E-06
$H_2PO_4^-$	2.4940E-13	8.9124E-14	4.1380E-13
SO_4^{2-}	3.2861E-02	8.3463E-04	5.4521E-02
HSO_4^-	2.9813E-15	3.0884E-15	4.9464E-15
CO_2(aq)	2.5409E-13	8.8279E-13	4.2157E-13
Solid solution			
$3CaO{\cdot}Al_2O_3{\cdot}6H_2O$	10^{-7}	10^{-7}	
$3CaO{\cdot}Al_2O_3{\cdot}3SiO_2$	0.0196	1.000	
Condensed solids			
$CaCO_3$	0.55383		
$Ca_5(PO_4)_3OH$	0.033341		
$Mg(OH)_2$	0.1555		
$Al(OH)_3$ (gibbsite)	0.13644		
$MgFe_2O_4$	0.025024		
$SrCO_3$	0.0020611		
$Co(OH)_2$	0.00022		
$Na_2U_2O_7$	0.01885		
Cancrinite[b]	0.019707		

[a]pH = 13.41; ionic strength = 5.407; ϕ (osmotic coefficient) = 0.7950.
[b]Formula: $Al_6Si_6Na_{7.68}(NO_3)_{1.68}H_{8.2}O_{28.1}$.

estimated and the values for OH^- and H_2O were chosen to satisfy charge and mass balances, respectively, in the supernatant and solids. In drying the solids, the water associated with the solids was determined to be 226 g/kg. We tacitly assumed that the supernatant was identical to this interstitial fluid and was in thermodynamic equilibrium with the sludge solids. In actual waste tanks, this is often not a good assumption. However, the sample described in Table 13 had been thoroughly mixed in the laboratory; hence, it was much more likely to be in equilibrium.

A comparison of the solid-liquid partitioning, given in Fig. 32, indicates reasonably good agreement with the analytical data. This partition assumes that liquid inventories are distributed to supernatant and wet solids according to the fraction of water in each. The elements and species expected to be completely in the solid phase are predicted to be so (i.e., Ca, Co, Fe, Mg, Si, Sr, U, PO_4^{3-}). The partitioning of Al, Na, and NO_3^- was predicted within a few percent (as is CO_3^{2-}, whose value was picked somewhat arbitrarily so as to match the solid phase data). For the remaining species (K, Br^-, Cl^-, F^-, and SO_4^{2-}), the calculated solutions varied—some match data well, while others grossly underpredicted solid-phase inventories. The modeling was quite incomplete for these species; all were assumed to be completely in solution and were partitioned to wet solids only in interstitial fluid.

Proposed treatment of sludges includes leaching with concentrated sodium hydroxide, which will hopefully dissolve certain metals and leave most radioactive species as precipitates. Experiments were performed on the ORNL sludge sample to ascertain the effectiveness of this plan in separating nonradioactive waste from the bulk solids. The sludge solids were centrifuged and decanted; then a small sample (36.72 g) was combined with 88.64 g of 3.14 *M* NaOH. After 144 h of mixing at room temperature, samples of both leachate and solids were analyzed; the results are shown in columns 3 and 4 of Table 15.

This process was simulated using the equilibrium model. Assuming 52% of the liquid inventories remain with the wet solids after decantation, the calculated inventories match measured values for most species, shown in columns 2 and 5 of Table 15. Noticeably erroneous are values for several constituents (K, Si, Cl, NO_3, and SO_4). Except for possibly silicon, these discrepancies are not likely to have a major impact on the calculated results. The fraction of aqueous inventories remaining in solids as interstitial fluid was determined so as to match the measured leachate sample weight of 83.35 g.

An initial equilibrium calculation produced the results given in column 5 of Table 15. As seen, there is a significant disparity in the calculated and measured values for aluminum in leachate. Several alternative calculations were attempted to ascertain the cause of this. Variation of the silicon inventory decreased the calculated value of aqueous aluminum only by 4%. A sensitivity analysis revealed high sensitivity to several free energies of formation, as shown in Table 16. In addition, the CO_3^{2-} inventory is rather uncertain due to the arbitrary manner in which it was originally chosen. A second calculation was performed in which the most sensitive free energies were changed within the uncertainty limits stated in Table 16 and the CO_3^{2-} concentration was decreased by 14%. The results, as shown in column 6 of Table 15, indicate good agreement with the measured value for leached aluminum.

The results in Table 15 do not match the data for several other components. The variation in results for potassium is consistent with the variation in input amounts; however, the variation for anions Cl^-, NO_3^- and SO_4^{2-} cannot be reconciled. The data indicate almost total recovery of SO_4^{2-}

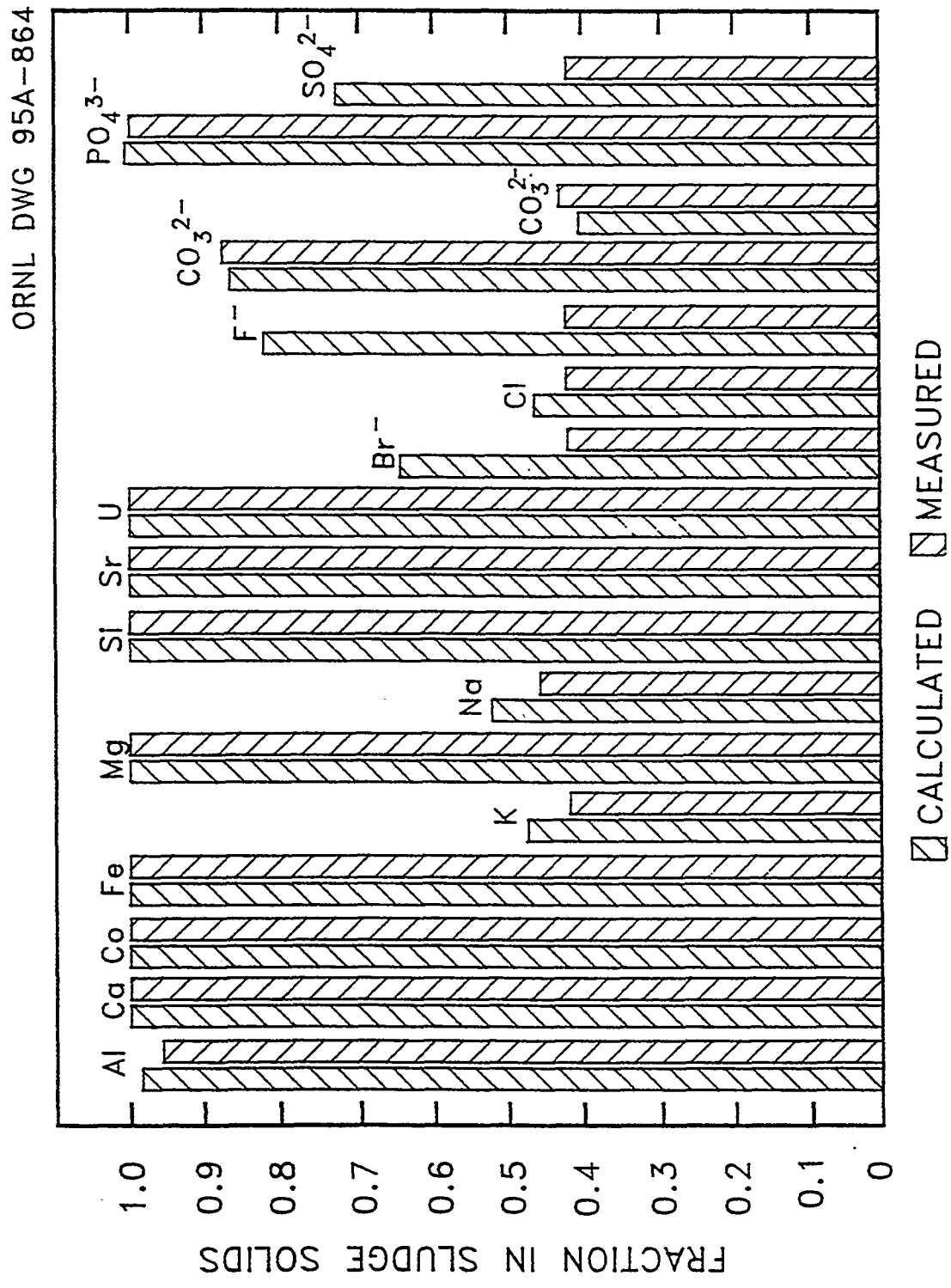

Fig. 32. Distribution of major components.

Table 15. Calculational results for caustic leaching (3.14 *M* NaOH)

	Wet solids (mg)		Sample leachate (mg)		
Component	Calculated	Data[a]	Data[a]	Original[b]	Alternative[c]
Al	554.4	559	4.3	149.5	4.8
Ca	2,098.1	2080	0.2	0.1	0.1
Co	0.9				
Fe	187.7	186	0.02		
K	345.4	312	192	236.9	237.4
Mg	294.7	292	0.1		
Na	2,545.2			5,707.7	5,720.0
Si	223.1	331	5.7		
Sr	12.2			0.4	0.3
U	602.6	598	0.9		
Br^-	12.4			8.5	8.5
Cl^-	90.6	80	22.7	62.1	62.3
F^-	26.4			18.1	18.1
CO_3^{2-}	2,585.0			978.6	1,383.8
NO_3^-	5,164.5	3810	840	3,542.6	3,550.3
PO_4^{3-}	641.1	639	0.7	7.4	9.5
SO_4^{2-}	110.3	152	149.3	75.6	75.8
OH^-	174.0			2,626.4	2,494.0
H_2O	21,051.5			69,936.0	69,785.2
Total				83,350.0	83,350.1

[a]Values taken from ref. 38.
[b]Assuming that 68.6% of the aqueous species was recovered in the leachate.
[c]Assuming that 68.7% of the aqueous species was recovered in the leachate.

Table 16. Sensitivity analysis of aluminate ion to free energies of formation

Species	Reduced chemical potential (μ^0/RT)			
	Nominal value[a,b]	Uncertainty[b]	Alternate value[c]	Sensitivity[d]
H_2O	–95.667	0.016	–95.651	–53.5
CO_3^{2-}	–212.964	0.161	–213.125	80.8
$Al(OH)_4^-$	–526.65	0.5	–526.15	–102.1
OH^-	–63.417	0.04	–63.377	–36.4
$3CaO{\cdot}Al_2O_3{\cdot}6H_2O$	–2,022.875	3	–2,025.875	7.5
$CaCO_3$	–455.487	0.403	–455.084	–172.8
$Ca_5(PO_4)_3OH$	–2,535.920	2.017	–2,533.903	–2.3
$4CaO{\cdot}Al_2O_3{\cdot}13H_2O$	–2,964.380	5	–2,969.380	276.1

[a]Used in calculating values shown in column 5 of Table 15.

[b]Uncertainties for H_2O, CO_3^{2-}, OH^-, $CaCO_3$, and $Ca_5(PO_4)_3OH$ were taken from original sources of nominal values. Uncertainties for remaining species were estimated (1) from the variations in literature of nominal values and (2) by comparison with similar species.

[c]Obtained from the nominal value by adding or subtracting uncertainty, depending on sign of sensi CO_3^{2-} tivity, and used to calculate values shown in column 6 of Table 15.

[d]Proportional rate of change, assuming nominal equilibrium. The sensitivity represents the percent change in $Al(OH)_4^-$ ion concentration, given a 1% change in parameter value.

in the leachate, which suggests that this component exists totally as an aqueous ion and that virtually all liquid (i.e., 98%) is recovered as leachate. The NO_3^- and Cl^- values suggest that substantial quantities are retained in the solids or interstitial liquid. In the former case, this would require a high retention of cations by solids as well (chiefly sodium, which was not measured) and is not realistic. The latter case would suggest that only 20–30% of the liquid was decanted, which contradicts the results for SO_4^{2-}. In most cases, decanted liquid comprises 40–60% of the total liquid. Evidently, some of the difficulty lies in erroneous data.

The system may well be sensitive to other quantities as well. Only two inventories (silicon and CO_3^{2-}) were evaluated, but others could also be important. A number of ion interaction parameters, including those that characterize carbonate interactions with nitrate, aluminate, and sulfate are not known and, therefore, are presumed to be zero. Finally, even the form of certain solids is uncertain. Table 16 indicates high sensitivity to $CaCO_3$ free energy. While the assumed form is calcite, it is possible that some aragonite could also be present. In the latter case, the $CaCO_3$ chemical potential should be altered so as to favor lower aluminum in solution.

It is somewhat unsatisfying that the calculated value for aluminum in leachate could only be reconciled by altering input parameters. This clearly illustrates the limitations in modeling such a complex system. Perhaps a complete model, in which all ion interactions were well characterized and all free energies were calibrated to solubility data, would fare better. In the present case, it is certainly essential that CO_3^{2-} interactions be improved, not to mention those for SO_4^{2-}, Mg^{2+}, and PO_4^{3-}.

However, the same difficulties encountered in modeling are precisely those that would be encountered in actual process design. There are tremendous uncertainties in the species present as well as the behavior of those species under various treatment options. Many such species (e.g., Ca, CO_3^{2-}) do not, at first glance, appear to be important in caustic leaching, which seeks primarily to convert $Al(OH)_3$ (gibbsite) to $Al(OH)_4^-$ (aq) (aluminate). Thus, as limited as it is in calculating precise solid-liquid separation, the combination of equilibrium modeling and a comprehensive sensitivity analysis is quite useful in the evaluation of various sludge processing strategies.

6. MODELING URANIUM HYDROLYSIS

In mildly acidic solution, it is widely recognized that uranium(VI) hydrolyzes extensively. This reaction has been confirmed from a number of experiments that measure the consumption of OH^- (or formation of H^+) in various salt solutions containing initial known amounts of UO_2^{2+} (see ref. 39 for an extensive survey of experiments performed over the past 50 years). It is universally assumed that all changes in OH^- (or H^+) levels can be accounted for by complexation with uranyl ions according to the general reaction

$$mUO_2^{2+} + nH_2O \leftrightarrow (UO_2)_m(OH)_n^{2m-n} + nH^+ . \qquad (18)$$

For the most part, the data come in the form of pH measurements, and sophisticated fitting routines have been used to estimate the equilibria for various choices of m and n in Eq. (18). In addition, spectrographic methods have sometimes been used to validate the presence or absence of various conjectured species.[40] For convenience, the uranium complex on the right of Eq. (18) will be referred to as U_{mn}.

The monograph by Baes and Mesmer[41] noted, nearly 20 years ago, that the dominant hydrolytic species were U_{22} and U_{35}. The presence of additional minor species was much more speculative, and their effects were often indistinguishable from nonideality variations. In chloride solutions, the form U_{34} has been noted, but more recent analyses infer that the complex U_{35} with Cl^- substituted for one of the OH^- groups (hereafter referred to as $U_{34}Cl$).

In addition to extensive hydrolysis experiments, isopiestic data were available for solutions of $UO_2(NO_3)_2$, UO_2Cl_2, and $UO_2(ClO_4)_2$.[42] Activity coefficients have been obtained from these data, assuming total dissociation to UO_2^{2+} and anions and essentially ignoring hydrolysis. The Pitzer semi-empirical model for activity coefficients has been fit to such data, again assuming complete dissociation. The Pitzer model has frequently been used in cases where complexing is known to occur, and under certain conditions it may suffice. It should be suspect, however, when the presence of additional solution components is likely to affect complexing (e.g., when pH is varied in the acidic region).

Thus, we desired to construct a model that uses both the wealth of hydrolysis data and the isopiestic measurements to thoroughly characterize uranium(VI) behavior in aqueous solutions. This was done by simultaneously fitting the binary Pitzer parameters for all major species likely to be present (listed in column 1 of Table 17). Standard free energies of formation were taken from ref. 39.

We recognized a priori that the only available data were a series of pH measurements (hydrolysis experiments) and water activities (isopiestic experiments). Total amounts of uranyl are known, but no direct measurements of either concentration or activity for any uranyl species are available. Thus, the calculation of activity coefficients and equilibrium amounts for these species would probably have greater uncertainties than if direct data were available.

References for the specific data (622 independent equilibrium measurements in Cl^- and NO_3^- media) are listed in Table 18. The Pitzer parameters for each anion were fit separately, assuming that all ternary interaction parameters were zero.

Results of this process are shown in Table 17, where the binary parameters are listed for each uranyl species. Recalculation of the equilibrium constants (log 10) for the reactions represented by Eq. (18) yielded the following values:

m,n	$(K_{m,n})$	
	This study	Literature[39]
2,2	–5.58	–5.62
3,5	–15.46	–15.55

When these values are compared with those of an earlier comprehensive study, agreement is quite good. The complex $U_{34}Cl$ is present in such small quantities that it could well have been omitted from this study. Evidently, the data used were not sufficient to characterize this species; therefore, the Pitzer parameters in Table 17 for this species should be regarded as highly suspect.

The present hydrolysis data cover the ionic strength range $0.5 < I < 3$ and involve the anions Cl^- and NO_3^-. A small number of data points at higher ionic strengths could be used to extend these results. In addition, the results of many experiments performed with the ClO_4^- anion at a range of ionic strengths, which have not been included in this study, should be considered in further efforts of this type.

The inclusion of additional experimental data would probably yield different Pitzer parameters. Furthermore, incorporation of data uncertainties would provide different weighting of individual data points, again producing different results. Nevertheless, the present parameter values are useful in simulating uranyl complex formation under the conditions used for our experiments.

Table 17. Estimation of parameters for aqueous uranyl complexes

		Binary Pitzer parameters					
		NO_3^-			Cl^-		
Species	μ_f^0	β^0	β^1	C	β^0	β^1	C
UO_2^{2+}	–384.469[a]	0.4523	1.5586	–0.0359	0.8599	–0.0130	–0.0932
U_{22}	–947.419[a]	–0.1677	2.3970	0.0162	–28.02	93.03	5.262
U_{35}	–1596.155[a]	4.529	–21.4395	–0.6908	2.0203	–8.2155	–0.3591
$U_{34}Cl$	–1561.807[a]				–2.7853	9.8022	0.2654

[a]Values taken from ref. 39.

Table 18. References for data used to construct model

Reference	Description of data
42	81 vapor pressure (isopiestic) measurements in $UO_2(NO_3)_2$ and UO_2Cl_2 binary solutions, ranging from 0.1 to 3.2 *M*
43	79 pH measurements in ~1 *M* NaCl; 2.8 < pH < 5.2; U_{TOT} = 1, 3, 10, 32; 101 mmol/L
44	54 pH measurements in 0.5 *M* KNO_3; 2.1 < pH < 5.1; 0.9 mmol/L < U_{TOT} < 20 mmol/L
45	189 pH measurements in 3 *M* NaCl; 2.1 < pH < 5.9; U_{TOT} = 80, 40, 20, 10, 5, 2.5, 1.25, 0.625 mmol/L
46	219 pH measurements in 0.5, 1, 1.5, 2, 2.5, 3 *M* $NaNO_3$; 2.2 < pH < 4.3; U_{TOT} = 100, 50, 25, 10, 5, 2.5, 1.3 mmol/L

7. REFERENCES

1. J. F. Zemaites, Jr., D. M. Clark, M. Rafal, and N. C. Scrivner, *Handbook of Aqueous Electrolyte Thermodynamics—Theory and Application*, A.I.Ch.E., Inc., New York, 1986.

2. B. Batchelor, *Models as Metaphors: The Role of Modeling in Pollution Prevention, Waste Man.* **14**, 243 (1994).

3. W. J. Hamer and Y. C. Wu, "Osmotic Coefficients and Mean Activity Coefficients of Uni-univalent Electrolytes in Water at 25°C," *J. Phys. Chem. Ref. Data* **1(4)**, 1047–99 (1972).

4. Y. C. Wu and W. J. Hamer, "Revised Values of the Osmotic Coefficients and Mean Activity Coefficients of Sodium Nitrate in Water at 25°C," *J. Phys. Chem. Ref. Data* **9(2)**, 513–18 (1980).

5. R. N. Goldberg, "Evaluated Activity and Osmotic Coefficients for Aqueous Solutions: Thirty-six Uni-Bivalent Electrolytes," *J. Phys. Chem. Ref. Data* **10(3)**, 671–764 (1981).

6. K. S. Pitzer, "Ion-Interaction Approach: Theory and Data Correlation," in K. S. Pitzer, ed., *Activity Coefficients in Electrolyte Solutions*, 2d ed., CRC Press, Boca Raton, Fla., 1991.

7. K. S. Pitzer, "Thermodynamics of Electrolytes. I. Theoretical Basis and General Equations," *J. Phys. Chem.* 77, 268 (1973).

8. H. T. Kim and W. J. Frederick, "Evaluation of Pitzer Ion Interaction Parameters of Aqueous Electrolytes at 25°C. 1. Single Salt Parameters," *J. Chem. Eng. Data* **33**, 177–84 (1988).

9. H. T. Kim and W. J. Frederick, "Evaluation of Pitzer Ion Interaction Parameters of Aqueous Mixed Electrolyte Solutions at 25°C. 2. Ternary Mixing Parameters," *J. Chem. Eng. Data* **33**, 278–83 (1988).

10. C. E. Harvie and J. H. Weare, *Geochim. Cosmochim. Acta* **44**, 981 (1980).

11. C. E. Harvie, H. P. Eugster, and J. H. Weare, *Geochim. Cosmochim. Acta* **46**, 1603 (1982).

12. C. E. Harvie, N. Moller, and J. H. Weare, *Geochim. Cosmochim. Acta* **48**, 723 (1984).

13. R. Fletcher, *Practical Methods of Optimization*, 2d ed., John Wiley & Sons, New York, 1987.

14. D. M. Young and R. T. Gregory, *A Survey of Numerical Mathematics*, Vol. I, Addison-Wesley, 1972.

15. I. Grenthe et al., *Chemical Thermodynamics of Uranium* (Final Draft), NEA-TDB, OECD Nuclear Energy Agency, Gif-sur-Yvette, France, 1990. See also D. Garvin, V. B. Parker, and H. J. White, *CODATA Thermodynamic Tables*, Hemisphere, Wash., 1987.

16. R. A. Robinson and R. H. Stokes, *Electrolyte Solutions*, 2d ed., Butterworths, London, 1959.

17. R. A. Robinson and A. K. Covington, "The Thermodynamics of the Ternary System: Water–Potassium Chloride–Calcium Chloride at 25°C," *J. Res. Nat. Bur. Stand. Sect. A* **72**, 239 (1968).

18. M. A. Hamid and R. Das, *J. Indian Chem. Soc.* **7**, 881 (1930).

19. R. Flatt and P. Bocherens, "Sur le Système Ternaire Ca^{2+}-K^+-NO_3^--H_2O," *Helv. Chim. Acta* **45**, 187–95 (1962).

20. A. M. Amirova and R. A. Karimov, "Influence of Nitric Acid and Phosphoric Acids on Solubility in the Calcium Nitrate–Potassium Nitrate–Water System," *Russ. J. Inorg. Chem.* **26(3)**, 430–32 (1981) [Transl. from *Zh. Neorg. Khim.* **26**, 801–5 (1981)].

21. A. G. Bergman and L. V. Opredelenkova, "Solubility Polytherms of the Calcium Nitrate-Potassium Nitrate–Water and Calcium Nitrate–Potassium Chloride–Water Ternary Systems," *Russ. J. Inorg. Chem.* **14(8)**, 1144–46 (1969) [Transl. from *Zh. Neorg. Khim.* **14**, 2180 (1969)].

22. K. S. Pitzer, "Thermodynamics of Electrolytes. V. Effects of Higher-Order Electrostatic Terms," *J. Solution Chem.* **4(3)**, 249–65 (1975).

23. S. N. Smith, S. Sarada, and R. Palepu, "Activity Coefficients of $NaNO_3$ in (Mg, Ca, Sr, and Ba)$(NO_3)_2$ + H_2O Systems at 298K by emf Methods," *Can. J. Chem.* **71**, 384–89 (1993).

24. R. A. Robinson and V. E. Bower, "Properties of Aqueous Mixtures of Pure Salts. Thermodynamics of the Ternary System: Water–Sodium Chloride–Calcium Chloride at 25°C," *J. Res. Nat. Bur. Stand. Sect. A* **70A(4)**, 313–18 (1966).

25. A. N. Kirgintsev and A. V. Luk'yanov, "Isopiestic Investigation of Ternary Solutions. V. Ternary $NaNO_3$-$Ca(NO_3)_2$-H_2O, $NaNO_3$- $La(NO_3)_3$-H_2O, $NaNO_3$-$Th(NO_3)_4$-H_2O, NaCl-$CaCl_2$-H_2O, NaCl-$LaCl_3$-H_2O, and NaCl-$ThCl_4$-H_2O Solutions at 25°," *Russ. J. Phys. Chem.* **39(3)** 389–91 (1965) [Transl. from *Zh. Fiz. Khim.*].

26. R. N. Roy et al, "Activity Coefficients for the System HCl + $CaCl_2$ + H_2O at Various Temperatures," *J. Chem. Soc., Faraday Trans. 1* **78**, 1405–22 (1981).

27. R. Flatt and P. Bocherens, "Le Système Quaternaire Ca^{2+}-K^+-H^+-NO_3^--H_2O à 25°," *Helv. Chim. Acta* **45**, 198–212 (1962).

28. W. F. Linke, *Solubilities*, 4th ed., Vol. I, D. Van Nostrand Co., Princeton, New Jersey, 1958.

29. R. G. Bates, V. E. Bower, R. G. Canham, and J. E. Prue, "The Dissociation Constant of $CaOH^+$ from 0° to 40°C," *Trans. Faraday. Soc.* **55**, 2062-8 (1959).

30. J. Johnston and C. Grove, "The Solubility of Calcium Hydroxide in Aqueous Salt Solutions," *J. Am. Chem. Soc.* **53**, 3976–91 (1931).

31. L. B. Yeatts and W. Marshall, "Aqueous Systems at High Temperature. XVIII. Activity Coefficient Behavior of Calcium Hydroxide in Aqueous Sodium Nitrate to the Critical Temperature of Water," *J. Phys. Chem.* **71(8)**, 2541–50 (1967).

32. H. Bassett, Jr., and H. S. Taylor, "Calcium Nitrate. Part III. The Three-Component System: Calcium Nitrate-Lime-Water," *J. Chem. Soc.* (London) **105**, 1926–41 (1914).

33. F. K. Cameron and W. O. Robinson, "The System, Lime, Nitric Acid and Water," *J. Phys. Chem.* **11**, 273-78 (1907).

34. J. Milikan, "Die Oxyhaloide der alkalischen Erden. Gleichgewichte in ternären Systemen, II," *Z. Physik Chem.* **92**, 496–520 (1918).

35. M. A. d'Amselme, "Solubilité du sulfate de calcium hydraté dans le solutions de sel marin," *Bull. Soc. Chim.* **29(3)**, 936–39 (1903).

36. N. Fratini, "Solubilitá dell'idrato di calcio in presenza di idrato di potassio e idrato di sodio," *Ann. Chim. Applicate* **39**, 616–20 (1949).

37. J. L. Collins et al., *Evaluation of Selected Ion Exchangers for the Removal of Cesium from MVST W-25 Supernate*, ORNL/TM-12938, Martin Marietta Energy Systems, Inc., Oak Ridge Natl. Lab., April 1995.

38. J. L. Collins et al., *Characterization and Leaching of Sludge form Melton Valley Storage Tank W-25*, TTP No. OR-1320-08, Oak Ridge National Laboratory, September 30, 1994.

39. I. Grenthe et al., *Chemical Thermodynamics of Uranium*, OECD Nuclear Energy Agency, 1992.

40. C. Nguyen-Trung, G. M. Begun, and D. A. Palmer, "Aqueous Uranium Complexes. 2. Raman Spectroscopic Study of the Complex Formation of the Dioxouranium (IV) Ion with a Variety of Inorganic and Organic Ligands," *Inorg. Chem.* **31(25)**, 5280–87 (1992).

41. C. F. Baes, Jr., and R. E. Mesmer, *The Hydrolysis of Cations*, Wiley & Sons, New York, 1976.

42. R. A. Robinson and C. K. Lim, "The Osmotic and Activity Coefficients of Uranyl Nitrate, Chloride, and Perchlorate at 25°C," *J. Chem. Soc.* 1840–43 (1951).

43. R. M. Rush, J. S. Johnson, and K. A. Kraus, "Hydrolysis of Uranium (VI): Ultracentrifugation and Acidity Measurements in Chloride Solutions," *Inorg. Chem.* **1(2)**, 378–86 (1962); see also R. M. Rush, J. S. Johnson, and K. A. Kraus, *Hydrolysis of U(IV): Acidity Measurements in Chloride Solutions and Absorption Spectra in Chloride and Perchlorate Solutions*, ORNL-3278, February 7, 1963.

44. C. F. Baes and N. J. Meyer, "Acidity Measurements at Elevated Temperatures. 1. Uranium (VI) Hydrolysis at 25 and 94°C," *Inorg. Chem.* **1(4)**, 780–89 (1962).

45. H. S. Dunsmore and L. G. Sillen, "Studies on the Hydrolysis of Metal Ions. 47. The Uranyl Ion in 3 *M* (Na)Cl Medium," *Acta Chem. Scand.* **17(10)**, 2657–63 (1963).

46. N. B. Milic and T. M. Suranji, "Hydrolysis of the Uranyl Ion in Sodium Nitrate Medium," *Z. Anorg. Alig. Chem.* **489**, 197–203 (1982).

47. R. Kremann and A. Zitek, "Die Bildung von Konversionssalpeter aus Natronsalpeter und Pottasche von Standpunkt der Phasenlehre," *Monatsh.* **30**, 311-40 (1909).

APPENDIX. THERMOCHEMICAL DATA

Free energies of formation for various electrolytes and ions have been obtained from the open literature (see Table A.1). In cases where the chemical potential was an optimizable parameter, the optimal values were used in all subsequent work.

Ion interaction parameters (i.e., Pitzer parameters), given in Table A.2, were obtained from a variety of sources, principally from ref. 6 and other work cited therein. The values obtained in Sect. 4 of this study are also included.

Table A.1. Free energies of formation

	μ^0/RT		μ^0/RT
Solid phase			
$Na_2SO_4 \cdot 10H_2O$	–1470.060	$Co(OH)_2$	–183.272
$Ca(OH)_2$	–361.910	$CoSO_4$	–315.593
$CaCO_3$ (calcite)	–455.487	$CoSO_4 \cdot 7H_2O$	–997.987
$CaCO_3 \cdot H_2O$	–549.294		
$CaSO_4 \cdot 0.5H_2O$	–579.631	$UO_2(OH)_2$	–564.261
$CaSO_4 \cdot 2H_2O$	–725.103	$UO_3 \cdot 2H_2O$	–659.790
$Ca_3(PO_4)_2$	–1567.190	UO_2CO_3	–630.542
$CaHPO_4 \cdot 2H_2O$	–869.264	UO_2SO_4	–680.082
$Ca(H_2P)_2 \cdot H_2O$	–1233.821	Na_2UO_4	–717.801
$Ca_5(PO_4)_3OH$	–2535.920	$Na_2U_2O_7$	–1214.890
$Mg(OH)_2$	–336.248	SiO_2 (quartz)	–345.504
$MgCO_3$	–415.429	$3CaO \cdot Al_2O_3 \cdot 3SiO_2$	–2533.628
$Mg_2(OH)_2(CO_3)$	–1036.114	Cancrinite	–5454.572
$CaMg(CO_3)_2$	–872.834	Montmorillonite	–2106.971
$MgSO_4 \cdot 7H_2O$	–1158.300		
$MgSO_4 \cdot H_2O$	–576.403	*Gas phase*	
$Mg_3(PO_4)_2$	–1428.580	Ar	0.000
		CO_2	–159.095
$Al(OH)_3$ (gibbsite)	–465.545		
AlOOH (boehmite)	–360.509	*Aqueous phase*	
Al_2O_3 (corundum)	–638.328	H_2O	–95.667
$NaAlCO_3(OH)_2$	–720.500	Na^+	–105.695
$MgAl_2O_4$	–877.377	K^+	–113.965
$Al_2(SO_4)_3 \cdot 6H_2O$	–1865.450	Ca^{2+}	–223.009
$KaI(SO_4)_2 \cdot 12H_2O$	–2074.250	Mg^{2+}	–183.716
$3CaO \cdot Al_2O_3 \cdot 6H_2O$	–2022.875	Al^{3+}	–198.279
$3CaO \cdot Al_2O_3 \cdot 13H_2O$	–2964.380	Fe^{3+}	–1.856
$AlPO_4$	–652.730	Sr^{2+}	–227.487
		Co^{2+}	–21.946
Fe_2O_3	–298.384	H^+	0.000
FeOOH	–197.561	UO_2^{2+}	–399.020
$Fe(OH)_3$	–280.975	NO_3^-	–44.700
$Fe_2(SO_4)_3$	–906.445	Cl^-	–52.928
		CO_3^{2-}	–212.964
$FePO_4 \cdot 2H_2O$	–668.778	HCO_3^-	–236.725
$MgFe_2O_4$	–545.049	$Al(OH)_4^-$	–526.650
$CaFe_2O_4$	–569.946	OH^-	–63.417
$3CaO \cdot Fe_2O_3 \cdot 6H_2O$	–1662.300	PO_4^{3-}	–413.664
$3CaO \cdot Fe_2O_3 \cdot 13H_2O$	–2603.820	HPO_4^{2-}	–442.146
		$H_2PO_4^-$	–458.766
$SrCO_3$	–458.962	SO_4^{2-}	–300.142
$SrSO_4$	–543.310	HSO_4^-	–304.701
$Sr(OH)_2$	–355.452	CO_2	–155.719

Table A.2. Ion interaction parameters

Parameter	Value	Interacting ions	Parameter	Value	Interacting ions
θ	0.0120	Na^+ K^+	β^0	0.0454	Na^+ HSO_4^-
θ	–0.0100	Na^+ Ca^{2+}	β^1	0.398	Na^+ HSO_4^-
θ	0.0700	Na^+ Mg^{2+}	C	0.0000	Na^+ HSO_4^-
θ	–0.019	Na^+ Co^{2+}			
θ	–0.069	Na^+ UO_2^{2+}	β^0	0.1781	Na^+ PO_4^{3-}
θ	0.0360	Na^+ H^+	β^1	3.8513	Na^+ PO_4^{3-}
			C	–0.0149	Na^+ PO_4^{3-}
θ	0.0050	K^+ H^+	β^0	–0.05828	Na^+ HPO_4^{2-}
θ	–0.0117	K^+ Ca^{2+}	β^1	1.4655	Na^+ HPO_4^{2-}
θ	0.0000	K^+ Mg^{2+}	C	0.0104	Na^+ HPO_4^{2-}
θ	0.0070	Ca^{2+} Mg^{2+}			
θ	0.0682	Ca^{2+} H^+	β^0	–0.0533	Na^+ $H_2PO_4^-$
θ	0.1000	Mg^{2+} H^+	β^1	0.0396	Na^+ $H_2PO_4^-$
θ	0.0642	Sr^{2+} H^+	C	0.0040	Na^+ $H_2PO_4^-$
β^0	0.0068	Na^+ NO_3^-	β^0	–0.0816	K^+ NO_3^-
β^1	0.1783	Na^+ NO_3^-	β^1	0.0494	K^+ NO_3^-
C	–0.00036	Na^+ NO_3^-	C	0.0033	K^+ NO_3^-
β^0	0.0864	Na^+ OH^-	β^0	0.1298	K^+ OH^-
β^1	0.2530	Na^+ OH^-	β^1	0.3200	K^+ OH^-
C	0.0022	Na^+ OH^-	C	0.0020	K^+ OH^-
β^0	0.0765	Na^+ Cl^-	β^0	0.05957	K^+ Cl^-
β^1	0.2664	Na^+ Cl^-	β^1	0.1782	K^+ Cl^-
C	0.00064	Na^+ Cl^-	C	–0.00433	K^+ Cl^-
β^0	0.0362	Na^+ CO_3^{2-}	β^0	0.1228	K^+ CO_3^{2-}
β^1	1.51	Na^+ CO_3^{2-}	β^1	1.433	K^+ CO_3^{2-}
C	0.0052	Na^+ CO_3^{2-}	C	0.0005	K^+ CO_3^{2-}
β^0	0.0280	Na^+ HCO_3^-	β^0	–0.0107	K^+ HCO_3^-
β^1	0.044	Na^+ HCO_3^-	β^1	0.0478	K^+ HCO_3^-
C	0.0000	Na^+ HCO_3^-	C	0.0000	K^+ HCO_3^-
β^0	0.0453	Na^+ $Al(OH)_4^-$	β^0	0.0500	K^+ SO_4^{2-}
β^1	0.3068	Na^+ $Al(OH)_4^-$	β^1	0.779	K^+ SO_4^{2-}
C	–0.00016	Na^+ $Al(OH)_4^-$	C	0.0000	K^+ SO_4^{2-}
β^0	0.0196	Na^+ SO_4^{2-}	β^0	–0.0003	K^+ HSO_4^-
β^1	1.113	Na^+ SO_4^{2-}	β^1	0.1735	K^+ HSO_4^-
C	0.0000	Na^+ SO_4^{2-}	C	0.0000	K^+ HSO_4^-

Table A.2. (continued)

Parameter	Value	Interacting ions	Parameter	Value	Interacting ions
β^0	0.3119	Co^{2+} NO_3^-	β^0	0.1346	Sr^{2+} NO_3^-
β^1	1.6905	Co^{2} NO_3^-	β^1	1.380	Sr^{2+} NO_3^-
C	–0.00269	Co^{2} NO_3^-	C	–0.00704	Sr^{2+} NO_3^-
β^0	0.3643	Co^{2+} Cl^-	β^0	0.2858	Sr^{2+} Cl^-
β^1	1.4750	Co^{2+} Cl^-	β^1	1.6672	Sr^{2+} Cl^-
C	–0.00538	Co^{2+} Cl^-	C	–0.00046	Sr^{2+} Cl^-
β^0	0.1631	Co^{2+} SO_4^{2-}	β^0	0.220	Sr^{2+} SO_4^{2-}
β^1	3.346	Co^{2+} SO_4^{2-}	β^1	2.880	Sr^{2+} SO_4^{2-}
β^2	–30.70	Co^{2+} SO_4^{2-}	β^2	–41.80	Sr^{2+} SO_4^{2-}
C	0.00926	Co^{2+} SO_4^{2-}	C	0.00475	Sr^{2+} SO_4^{2-}
β^0	0.2108	Ca^{2+} NO_3^-	β^0	0.3729	K^+ PO_4^{3-}
β^1	1.409	Ca^{2+} NO_3^-	β^1	3.972	K^+ PO_4^{3-}
C	–0.02014	Ca^{2+} NO_3^-	C	–0.02506	K^+ PO_4^{3-}
β^0	–0.2169	Ca^{2+} OH^-	β^0	0.02475	K^+ HPO_4^{2-}
β^1	0.06968	Ca^{2+} OH^-	β^1	1.2743	K^+ HPO_4^{2-}
β^2	–9.372	Ca^{2+} OH^-	C	0.0058	K^+ HPO_4^{2-}
β^0	0.3053	Ca^{2+} Cl^-	β^0	–0.0678	K^+ $H_2PO_4^-$
β^1	1.7805	Ca^{2+} Cl^-	β^1	–0.1042	K^+ $H_2PO_4^-$
C	0.00076	Ca^{2+} Cl^-	C	0.	K^+ $H_2PO_4^-$
β^0	0.3998	Ca^{2+} HCO_3^-	β^0	0.4607	UO_2^{2+} NO_3^-
β^1	2.9775	Ca^{2+} HCO_3^-	β^1	1.6130	UO_2^{2+} NO_3^-
C	0.0000	Ca^{2+} HCO_3^-	C	–0.00310	UO_2^{2+} NO_3^-
β^0	0.2000	Ca^{2+} SO_4^{2-}	β^0	0.4274	UO_2^{2+} Cl^-
β^1	3.1973	Ca^{2+} SO_4^{2-}	β^1	1.6440	UO_2^{2+} Cl^-
C	–54.24	Ca^{2+} SO_4^{2-}	C	–0.01303	UO_2^{2+} Cl^-
β^0	0.3671	Mg^{2+} NO_3^-	β^0	0.3220	UO_2^{2+} SO_4^{2-}
β^1	1.585	Mg^{2+} NO_3^-	β^1	1.827	UO_2^{2+} SO_4^{2-}
C	–0.00729	Mg^{2+} NO_3^-	β^2	–40.	UO_2^{2+} SO_4^{2-}
			C	–0.0044	UO_2^{2+} SO_4^{2-}
β_0	0.3524	Mg_{2+} Cl-			
β^1	1.6815	Mg^{2+} Cl^-	β^0	0.1168	H^+ NO_3^-
C	0.00184	Mg^{2+} Cl^-	β^1	0.3546	H^+ NO_3^-
			C	–0.0027	H^+ NO_3^-
β^0	0.033	Mg^{2+} HCO_3^-			
β^1	0.8498	Mg^{2+} HCO_3^-	β^0	0.1775	H^+ Cl^-
C	0	Mg^{2+} HCO_3^-	β^1	0.2945	H^+ Cl^-
			C	0.0004	H^+ Cl^-
β^0	0.215	Mg^{2+} SO_4^{2-}			
β^1	3.365	Mg^{2+} SO_4^{2-}	β^0	0.2103	H^+ HSO_4^-
β^2	–32.74	Mg^{2+} SO_4^{2-}	β^1	0.4711	H^+ HSO_4^-
C	0.0070	Mg^{2+} SO_4^{2-}	C	0	H^+ HSO_4^-

Table A.2. (continued)

Parameter	Value	Interacting ions		
θ	–0.0547	NO_3^-	OH^-	
θ	0.0160	NO_3^-	Cl^-	
θ	–0.05	OH^-	Cl^-	
θ	0.014	OH^-	$Al(OH)_4^-$	
θ	–0.02	Cl^-	CO_3^{2-}	
θ	0.03	Cl^-	HCO_3^-	
θ	0.03	Cl^-	SO_4^{2-}	
θ	–0.006	Cl^-	HSO_4^-	
θ	0.1	Cl^-	$H_2PO_4^-$	
θ	0.02	SO_4^{2-}	CO_3^{2-}	
θ	0.01	SO_4^{2-}	HCO_3^-	
θ	–0.013	SO_4^{2-}	OH^-	
θ	–0.04	CO_3^{2-}	HCO_3^-	
θ	0.1	CO_3^{2-}	OH^-	
λ	0.1095	CO_2(aq)	Na^+	
λ	0.0607	CO_2(aq)	Ka^+	
λ	0.2130	CO_2(aq)	Ca^{2+}	
λ	–0.0425	CO_2(aq)	NO_3^-	
λ	–0.0106	CO_2(aq)	Cl^-	
λ	1.9108	CO_2(aq)	CO_2(aq)	
ψ	–0.0110	K^+	H^+	Cl^-
ψ	–0.0103	K^+	H^+	NO_3^-
ψ	–0.0126	K^+	Ca^{2+}	NO_3^-
ψ	0.0027	K^+	Ca^{2+}	OH^-
ψ	–0.0088	K^+	Ca^{2+}	Cl^-
ψ	–0.0220	K^+	Mg^{2+}	Cl^-
ψ	–0.0480	K^+	Mg^{2+}	SO_4^{2-}
ψ	–0.0032	K^+	NO_3^-	OH^-
ψ	–0.0031	K^+	NO_3^-	Cl^-
ψ	–0.0032	K^+	Cl^-	OH^-
ψ	–0.0040	K^+	Cl	CO_3^{2-}
ψ	–0.0150	K^+	Cl^-	HCO_3^-
ψ	–0.005	K^+	Cl	SO_4^{2-}
ψ	–0.1	K^+	Cl^-	$H_2PO_4^-$
ψ	–0.010	K^+	CO_3^{2-}	OH^-
ψ	–0.0090	K^+	CO_3^{2-}	SO_4^{2-}
ψ	–0.0500	K^+	SO_4^{2-}	OH^-
ψ	0.0677	K^+	SO_4^{2-}	HSO_4^-

Parameter	Value	Interacting ions		
ψ	–0.0060	Na^+	K^+	NO_3^-
ψ	–0.0041	Na^+	K^+	OH^-
ψ	0.0018	Na^+	K^+	Cl^-
ψ	0.003	Na^+	K^+	CO_3^{2-}
ψ	–0.003	Na^+	K^+	HCO_3^-
ψ	–0.01	Na^+	K^+	SO_4^{2-}
ψ	–0.0174	Na^+	Ca^{2+}	NO_3^-
ψ	–0.0270	Na^+	Ca^{2+}	OH^-
ψ	–0.0070	Na^+	Ca^{2+}	Cl^-
ψ	–0.0550	Na^+	Ca^{2+}	SO_4^{2-}
ψ	–0.0150	Na^+	Mg^{2+}	SO_4^{2-}
ψ	–0.0150	Na^+	Mg^{2+}	Cl^-
ψ	–0.0040	Na^+	H^+	Cl^-
ψ	–0.0027	Na^+	H^+	NO_3^-
ψ	–0.0174	Na^+	Co^{2+}	SO_4^{2-}
ψ	–0.0002	Na^+	NO_3^-	OH^-
ψ	–0.0060	Na^+	NO_3^-	Cl^-
ψ	–0.0060	Na^+	Cl^-	OH^-
ψ	–0.0085	Na^+	Cl^-	CO_3^{2-}
ψ	–0.0150	Na^+	Cl^-	HCO_3^-
ψ	0	Na^+	Cl^-	SO_4^{2-}
ψ	–0.006	Na^+	Cl^-	HSO_4^-
ψ	0	Na^+	Cl^-	$H_2PO_4^-$
ψ	–0.0048	Na^+	$Al(OH)_4^-$	OH^-
ψ	–0.0170	Na^+	CO_3^{2-}	OH^-
ψ	0.0020	Na^+	CO_3^{2-}	HCO_3^-
ψ	–0.0050	Na^+	CO_3^{2-}	SO_4^{2-}
ψ	–0.0090	Na^+	SO_4^{2-}	OH^-
ψ	0.0050	Na^+	SO_4^{2-}	HCO_3^-
ψ	0.0094	Na^+	SO_4^{2-}	HSO_4^-
ψ	–0.0044	Ca^{2+}	H^+	NO_3^-
ψ	0.0577	Ca^{2+}	NO_3^-	OH^-
ψ	–0.0170	Ca^{2+}	NO_3^-	Cl^-
ψ	–0.0165	Ca^{2+}	Cl^-	OH^-
ψ	–0.002	Ca^{2+}	Cl^-	SO_4^{2-}
ψ	0.0240	Ca^{2+}	Mg^{2+}	SO_4^{2-}
ψ	0	Mg^{2+}	NO_3^-	Cl^-
ψ	–0.096	Mg^{2+}	Cl^-	HCO_3^-
ψ	–0.008	Mg^{2+}	Cl^-	SO_4^{2-}
ψ	–0.161	Mg^{2+}	SO_4^{2-}	HCO_3^-
ψ	–0.0425	Mg^{2+}	SO_4^{2-}	HSO_4^-

INTERNAL DISTRIBUTION

1-5. E. C. Beahm
6. B. Z. Egan
7. M. B. Emmett
8. R. D. Hunt
9. R. T. Jubin
10. M. A. Kuliasha
11. A. P. Malinauskas
12. C. P. McGinnis
13. L. F. Norris
14. J. M. Simonson
15. B. B. Spencer
16-20. C. F. Weber
21. T. D. Welch
22. R. M. Westfall
23-24. Laboratory Records Dept. Document Reference Section
25. Laboratory Records, ORNL-RC
26. Y-12 Technical Library
27. Central Research Library
28. ORNL Patent Section

EXTERNAL DISTRIBUTION

29. J. Appel, Westinghouse Hanford Co., P.O. Box 1970, G3-21, Richland, WA 99352
30. B. C. Bunker, Pacific Northwest National Laboratory, Battelle Boulevard, P.O. Box 999, K2-25, Richland, WA 99352
31. N. G. Colton, Pacific Northwest National Laboratory, Battelle Boulevard, P.O. Box 999, K2-25, Richland, WA 99352
32. A. R. Felmy, Pacific Northwest National Laboratory, Battelle Boulevard, P.O. Box 999, K2-25, Richland, WA 99352
33. K. Gasper, Westinghouse Hanford Co., P.O. Box 1970, G3-21, Richland, WA 99352
34. D. Geiser, U.S. Department of Energy, EM-52, Cloverleaf Building, 19901 Germantown Road, Germantown, MD 20874-1290
35. M. Hay, Westinghouse Savannah River Co., Savannah River Technical Center, Building 773A, Aiken, SC 29808
36. R. Kirkbride, Westinghouse Hanford Co., P.O. Box 1970, H5-27, Richland, WA 99352
37. G. J. Lumetta, Pacific Northwest National Laboratory, Battelle Boulevard, P.O. Box 999, P7-25, Richland, WA 99352
38. J. Noble-Dial, U.S. Department of Energy, Oak Ridge Operations Office, P.O. Box 2001, Oak Ridge, TN 37830
39-40. Office of Scientific and Technical Information, U.S. Department of Energy, P.O. Box 62, Oak Ridge, TN 37831
41. Office of the ORNL Site Manager, Department of Energy, Oak Ridge National Laboratory, P.O. Box 2008, Oak Ridge, TN 37831
42. R. Orme, Westinghouse Hanford Co., P.O. Box 1970, H5-27, Richland, WA 99352
43. T. Stewart, Pacific Northwest National Laboratory, Battelle Boulevard, P.O. Box 999, K9-91, Richland, WA 99352
44. J. Swanson, 1318 Cottonwood Dr., Richland, WA 99352

45. D. Temer, Los Alamos National Laboratory, P.O. Box 1663, MS J586, Los Alamos,NM 87545
46. M. Thompson, Westinghouse Savannah River Co., Savannah River Technical Center, Building 773A, Aiken, SC 29808
47. G. Vandegrift, Argonne National Laboratory, 9700 S. Cass Ave., Argonne, IL 60439
48. D. Washenfelder, Westinghouse Hanford Co., P.O. Box 1970, H5-27, Richland, WA 99352